Influence of Isospin Momentum Dependent Interactions on Transverse Flow

Dissertation submitted in partial fulfilment of the requirement for

The award of the degree of

Masters of Science

In

Physics

Under

The supervision of

Dr. Suneel Kumar

Submitted by

Amandeep Kaur

Roll No - 301104003

School of Physics and Material Science

Thapar University

Patiala – 147004 (PUNJAB)

INDIA

CERTIFICATE

I hereby declare that the report entitled "**Influence of Isospin Momentum Dependent Interactions on Transverse Flow**" is an authentic record of my own work carried out for the partial fulfilment of the requirement for the award of the degree of M.Sc. (Masters of Science) at Thapar University, Patiala (Punjab), under the guidance of Dr. Suneel Kumar (School of Physics and Materials Science). The matter presented in the dissertation has not been submitted in part or full for the award of any other degree.

Amandeep Kaur

Amandeep Kaur

Roll No. : 301104003

Date: 13-June-2013

It is certified that the above statement made by the candidate is correct to the best of my knowledge and belief.

S Kumar

(Dr. Suneel Kumar)

Associate Professor

School of Physics and Materials Science

Thapar University, Patiala

26/6/13

(Dr. Kulvir Singh)

(Head)

School of Physics and Materials Science

Thapar University, Patiala

27/6

(Dr. S.K. Mohpatra)

Dean of Academic

Affairs

Thapar University,

Patiala

ACKNOWLEDGEMENT

Foremost, I would like to express my sincere gratitude to my supervisor **Dr. Suneel Kumar** for his continuous support and supervision, for his patience, motivation, enthusiasm, and immense knowledge. His guidance helped me at all times of research and in writing this dissertation. I could not have imagined having a better advisor and mentor for my thesis.

I would like to thank **Dr. Kulvir Singh**, Head, School of Physics and Materials Science for his support and providing me the necessary lab facilities.

I express my deepest gratitude to **Mr. Karan Singh Vinayak and Miss Anupriya Jain**, without whom I would not have been able to complete my dissertation. My sincere thanks to the research scholars of the physics department for their help and valuable suggestions.

Special thanks to my friends **Sangeeta, Reema, Sahil, Mandeep**, **Navjot and Ajitpal** who helped me at every step during this work and staffs at the School of Physics and Material Sciences for providing me a friendly atmosphere and encouraging me throughout this work.

I am deeply thankful to my family, for their moral support and patience which gave me the necessary motivation and strength to endure research and complete my thesis.

Above all I render my gratitude to Almighty who bestowed me the strength and vision to walk on the path of truth.

Amandeep Kaur

Date: 13- June- 2013

Place: Thapar University, Patiala

Amandeep Kaur

Roll No. 301104003

ABSTRACT

We investigate the role of isospin momentum dependent interactions on directed transverse flow and its disappearance by inserting an isospin degree of freedom into the momentum dependent interactions using isospin quantum dependent quantum molecular dynamics model. This analysis carried out for the symmetric reactions of isotopic series of Ca+Ca and Xe+Xe at wide range of incident energies. We demonstrated the effect of momentum dependent interactions on directed transverse momentum in heavy-ion collisions at intermediate energies. The role of isospin in heavy-ion collisions is explored via momentum dependent interactions subjected to different equation of states (soft and hard). We studied the mass dependence of balance energy. It is found that the isospin momentum dependent interactions effect the balance energy.

CONTENTS

Chapter 2: Methodology

Chapter 3: Influence of Isospin Momentum Dependent Interactions on Directed Transverse In-Plane Flow

Chapter 1

Introduction

The science of nuclear physics deals with the properties of nuclear matter. The main interest revolves around the structure of nucleus and interactions among nucleons (protons and neutrons). The understanding of various nuclear phenomena is also vital for the understanding of the mechanism behind the nuclear reactions that fuel the stars, including our sun. Another domain of the interest in nuclear physics is to investigate the properties of nuclear matter at high densities and temperature [1]. The fundamental goal of the nuclear physics is to understand the properties of nuclear matter as well as of atomic nuclei and to explore how nuclei are built up from elementary constituents. Nuclear physics involves the study of the diverse phenomena at vastly different scales, from the interaction of the elementary entities (quarks and gluons) inside nucleons or nuclei, to formation of the elements via nuclear synthesis in stars and supernovae, or the characteristics of the hot and dense nuclear matter as it occurred during the early phase of the universe. This not only helps us to understand the basic properties of nuclei and interactions among the constituents but also contributes significantly to the society in the form of nuclear energy, nuclear medicine and therapy.

On the basis of energy of colliding nuclei, heavy ion physics can be classified in following branches [2].

i). Low energy heavy ion physics: **$E \leq 10$ MeV/nucleon**
ii). Intermediate energy heavy ion physics: **10 MeV/nucleon$<E<$2 GeV/nucleon**
iii). High energy heavy ion physics: **$E \geq 2$ GeV/nucleon**

1.1 Low Energy Heavy Ion Physics

The study at low energy heavy ion physics is to look for the low density phenomena. The low energy nuclear physics mainly focus on the structure of nuclei, fusion [3] and fission, cluster radioactivity, gamma (ɣ) ray spectroscopy and halo nuclei [4]. Fig. 1.1 shows schematic view of fusion process at low energy 5 MeV. Low energy physics focuses mainly on the structure of nuclei.

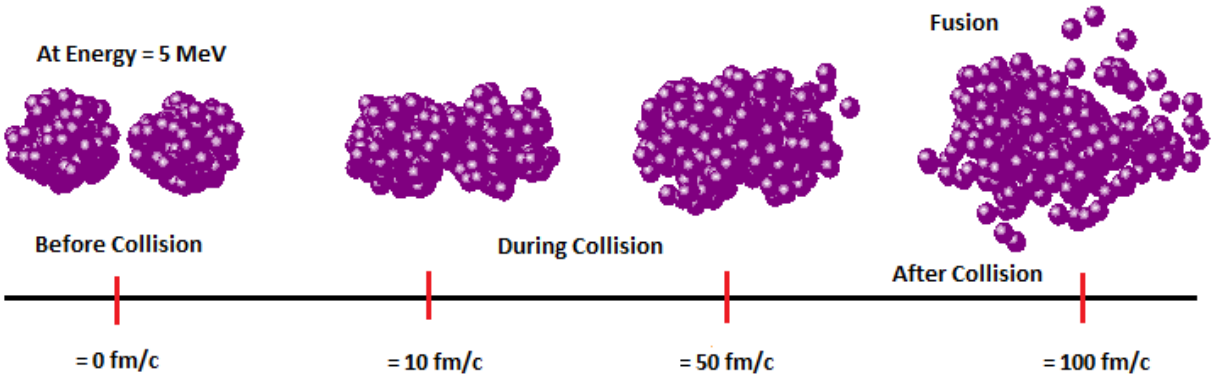

Fig. 1.1: Schematic view of fusion process at low energy (E = 5 MeV/nucleon)

Due to the lack of free phase space available at low incident energy, about 98% of the attempted collisions are blocked. Thus, dynamics at low energies is governed by the mean field only.

1.2 Intermediate Energy Heavy Ion Physics

Intermediate energy nuclear physics gives the possibilities to study the properties of nuclear matter under extreme conditions. The properties of nuclear matter, like all other materials, are also influenced by the pressure, density, and temperature. Various phenomena's that we study at intermediate energy nuclear physics are collective flow, multifragmentation, nuclear stopping and isospin physics etc. Fig. 1.2 shows schematic view of fragmentation process at intermediate energy 100 MeV/nucleon. In intermediate energy physics, both

mean field and nucleon-nucleon collision takes place. Reactions at intermediate energy range are violent enough to excite the system to very high temperature leading to the break-up of initial correlations among nucleons, but not enough to break the internal structure of nucleons or hadrons.

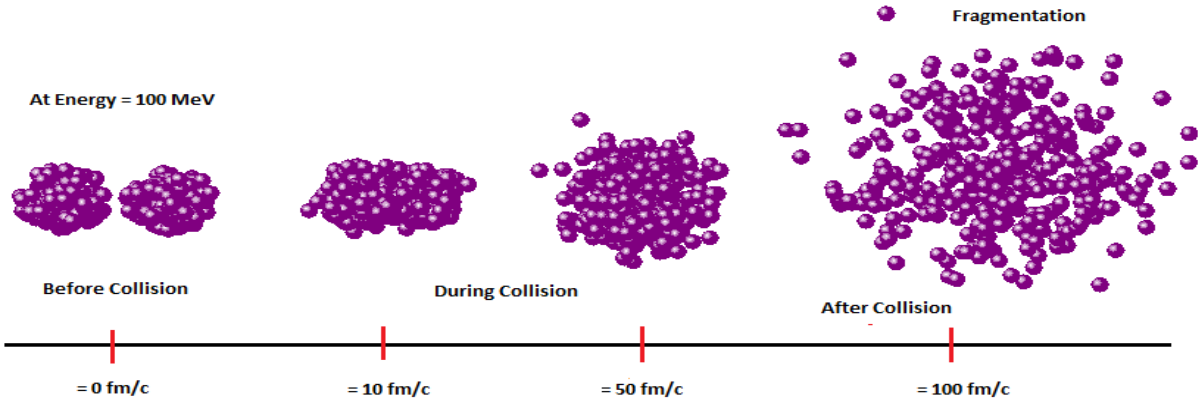

Fig. 1.2. Schematic view of collisions at intermediate energy (E = 100 MeV/nucleon)

1.3 High Energy Heavy Ion Physics

High energy nuclear physics is a field of study which deals with the properties of nuclear matter at energies greater than 2 GeV/nucleon. At very high densities and temperatures, one may have the quark gluon plasma [5]. Fig. 1.3 shows a schematic view of collision at high energy 5 GeV/nucleon. Various phenomena's that we study at high energy physics are fundamental particle production. The availability of large free phase-space at high energy makes the Pauli blocking role quite small (roughly 4% collisions are blocked) and hence the dynamics of a reaction is governed by the nucleon-nucleon collisions.

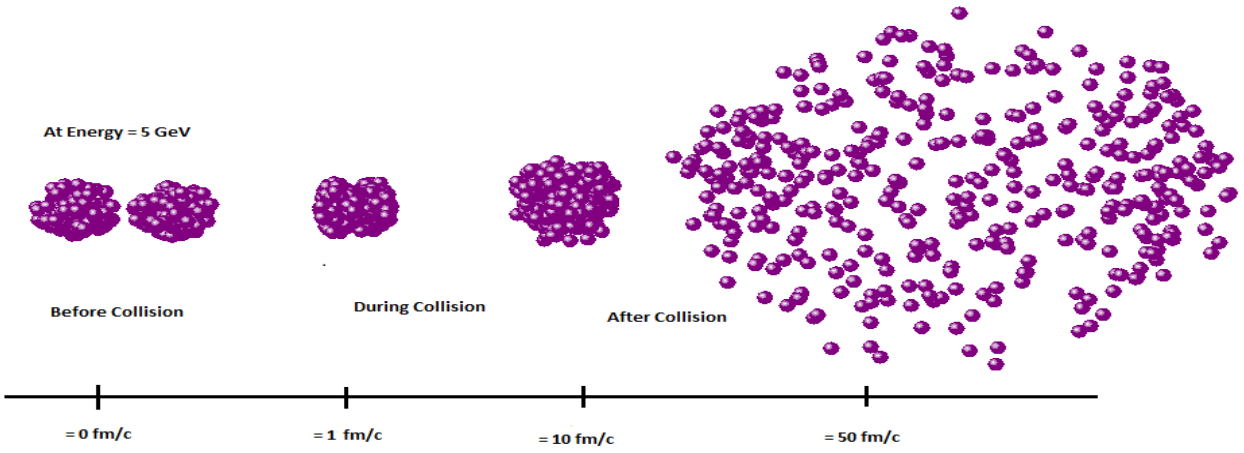

Fig. 1.3: Schematic view of collision at high energy (E = 5 GeV/nucleon)

1.4 Phase Diagram of Nuclear Matter

We find that the state of nuclear matter depends on temperature and density. In normal states at lowest energy, nuclei show liquid-like characteristics and have a density of 0.17 nucleons/fm^3. In more conventional units, this corresponds to 2.7×10^{17} kg/m^3, or 270 trillion times the density of liquid water. In fig. 1.4 the X-axis represents the scaled density, whereas temperature is shown on Y-axis. The normal nuclear matter (at $\rho = \rho_0$, T = 0) represents a liquid phase. The liquid-gas phase (LGP) transition region at the lower left corner of the figure is characterized by the temperature below ≈ 15 MeV and densities ($\rho/\rho_0 < 1$). The region of very high density and temperature corresponds to the Quark-Gluon Plasma (QGP) phase. The hadron gas (HG) phase exists at intermediate temperatures and densities. The neutron star (NS) density region extends from the low density up to more than 10 times the normal nuclear matter density. The typical temperatures are less than 10 MeV for newly born neutron stars and less than 0.01 MeV for cold neutron stars. The line that separates the QGP phase from the HG phase is the phase co-existence and/or transition region.

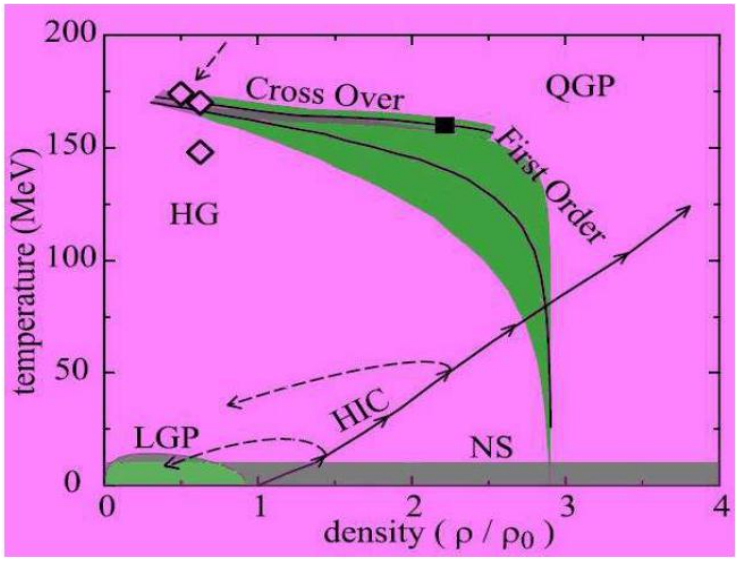

Fig. 1.4: The phase diagram for nuclear matter, as predicted theoretically. The horizontal axis shows the matter density, and the vertical axis shows the temperature. Both axes are shown on logarithmic scale, and the density is given in multiples of normal nuclear matter density. The figure is taken from reference [6].

In the study of hot dense matter, heavy-ion reactions offer excellent opportunities compared to other methods. The purpose of studying nuclear matter phase diagram is to understand the early history of our universe, and to understand high-density objects, called neutron stars in our present day universe. Though, the dense matter exists in the neutron stars, unfortunately, only indirect information can be extracted from the astrophysical observations. The QGP and dense hadron gas phases existed in the early stage of the evolution of universe (about 15 billion years ago) are inaccessible today. Depending on intial conditions, various densities and temperatures can be reached and thus a large scale exploration of the nuclear matter phase diagram is possible. Hence heavy ion collisions seem to offer a unique opportunity for exploring the phase diagram of nuclear matter.

1.5 Nuclear Equation of state (NEOS)

An equation of state (EOS) is a nontrivial relation between thermodynamic variables characterizing a medium. Nuclear equation of state gives the information about how much we can compress the nuclear matter at given energy. We can compress the nuclear matter by colliding two ions; it means we add the compressional energy into the system. Nuclear equation of state tells us that which compressional energy corresponds to which density. To achieve parameterization one uses the so-called Skyrme-ansatz and uses different parameter sets corresponding to different compressibility values ranging from about 200 MeV (less repulsive) a so-called soft EOS up to about 400 MeV (more repulsive) a so-called hard EOS. The corresponding compressional energy curves as shown in Fig. 1.5.

Apart from different equation of state, the momentum dependence of EOS has also attracted lot of considerations. One should, however, note that the compressibility depends not only on the density but also the entire momentum plane. In other words, equation of state apart from the population of nucleons also depends upon their relative velocities. These momentum dependent interactions, give rise to two new equations of state. A set with momentum dependence and soft equation of state is called SMD, whereas a hard equation of state with momentum dependence interaction is called HMD. These momentum dependent interactions are repulsive in nature. The nuclear EOS is of interest because it affects the fate of the Universe at times $t \geq 1\mu s$ from the Big Bang and because its features are behind the supernova explosions. Moreover, its features ensure the stability of neutron stars [7].

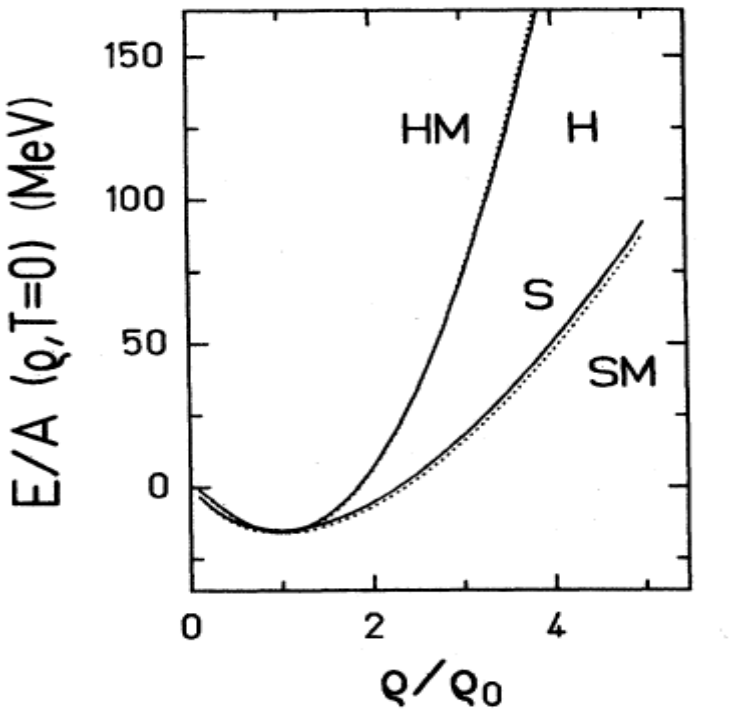

Fig. 1.5: The density dependence of the compression energy per particle. The hard,soft, HMD and SMD interactions are shown by solid, dash-dot-dash,dash-double-dotted and dashed lines,respectively.

1.6 Different Phenomenon at intermediate energies

1.6.1 Multifragmentation

It is the process when two nuclei collide, during this collision they break into several small and medium sized fragments and lot of nucleons are emitted as shown in Fig. 1.6. The particles which are produced includes free nucleons (FN's) [A = 1], light charged particles (LCP's) [$2 \leq A \leq 4$] as well as heavy clusters. A schematic view of multifragmentation is illustrated in Fig. 1.6.

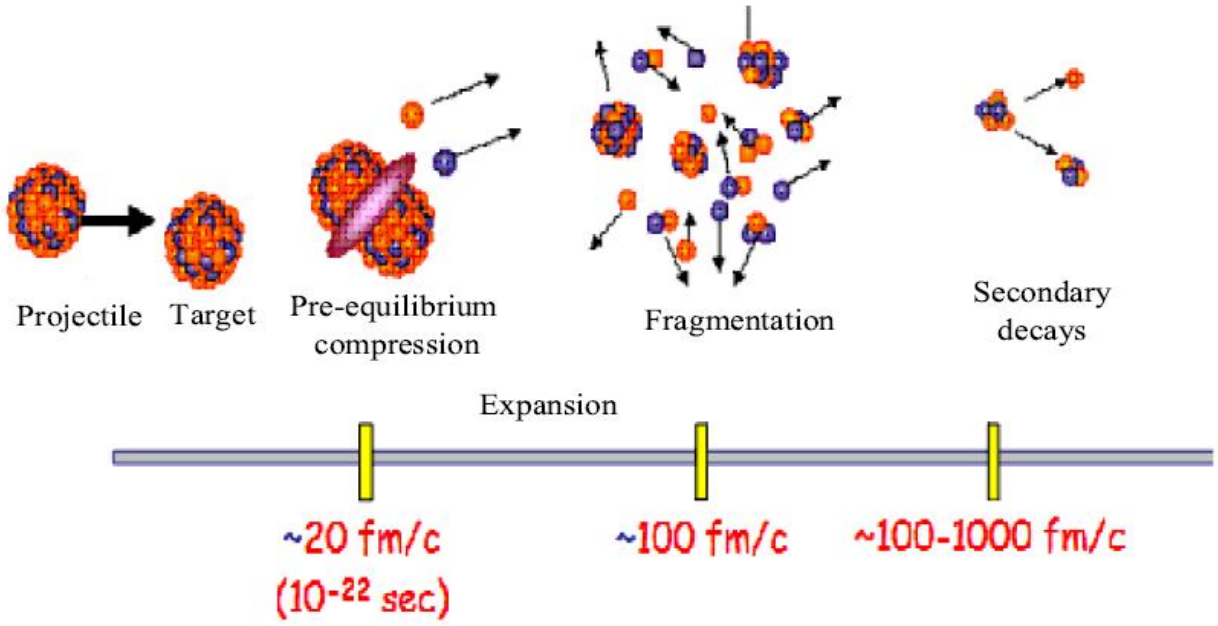

Fig. 1.6: A schematic view of multifragmentation.

1.6.2 Nuclear Stopping

Nuclear stopping [8] is one of the essential observable of thermalization that depends crucially on reaction dynamics. It has been linked with the degree of thermalization and equilibrium reached in a reaction. The global stopping is defined as the randomization of one-body momentum space. More the initial memory of nucleons erased, better it is stopped and better one has average mixing of projectile and target momentum. The destruction of initial correlations makes the matter homogenous and can have global stopping. During the collision of projectile and target, three possibilities arise:

(i) The nuclei are repelled like in the collisions of two hard spheres.

(ii) The nuclei are compressed and mix up like in the collision of two droplets.

(iii) And the nuclei are transparent to each other and passes without interactions like crowds of bees. These three different possibilities are shown in Fig. 1.7.

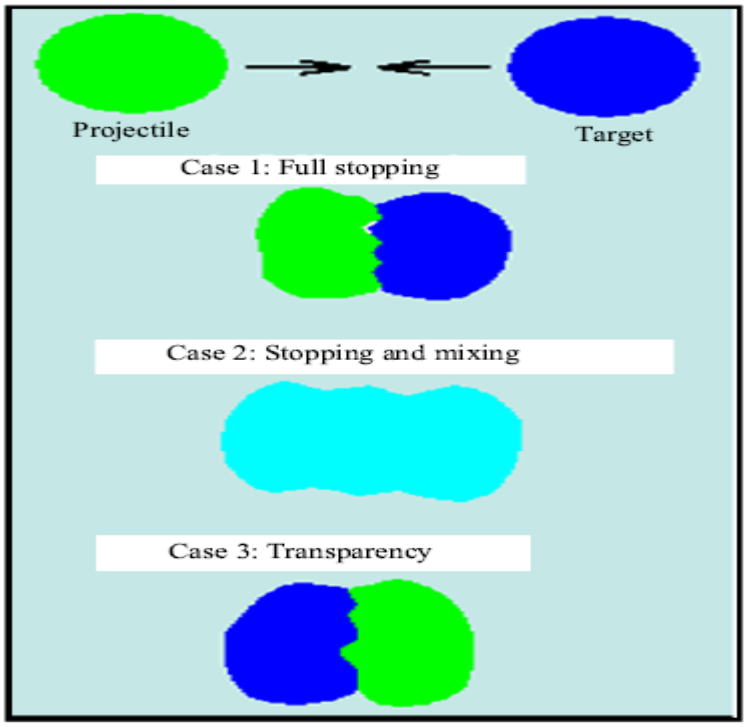

Fig. 1.7: A schematic view of movement of projectile and target. Three possibilities arise during different collisions depending on incident energies. Case 1: Full stopping, Case 2: Stopping and mixing and Case 3: Transparency.

1.6.3 Collective Flow

When two nuclei collide with each other at intermediate energies and are compressed to densities higher than ρ_o a flow pattern will develop as the system subsequently expands. During the decompression stage, the directions and speed of constituent particles are influenced by pressure gradients, i.e., particles tend to flow to regions of low pressure. This pressure-dependent correlation between particle positions and momenta is known as collective flow. The collective flow is a measure of the transverse motion imparted to particles and fragments during the collision of two nuclei. The development of collective flow is closely related to the pressure build-up during the compression stage of the reaction,

and gives us information about the pressure and particle density relation. Collective flow is of various types, namely, the radial flow, elliptic flow, directed flow, triangular flow and higher order anisotropic flows.

(a) Radial Flow

It arises in the central collisions and its existence is based on the increased yields in the kinetic energy spectra of the particles emitted near $\theta_{c.m.} = 90°$ relative to the beam axis. The review about the radial flow can be found in Ref. [9]. Fig. 1.8 shows the schematic view of radial flow observed in the central collision.

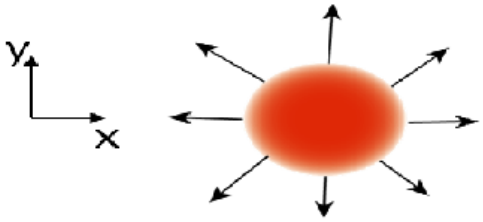

Fig. 1.8: Schematic view of radial flow observed in the central collision.

(b) Directed Transverse Flow

The Directed flow is a preferential emission of the particles within, and a particular side of reaction plane. It is the deflection of the nucleons and fragments to finite scattering angles [10]. Stated another way the phenomenon of different fragments or different particles deflected sideward from the hot and dense region formed by the overlap of projectile and target nuclei is called directed flow. The directed flow effects emission of the particles at forward and backward rapidities (at energies above a few hundred MeV/nucleon). The particles get deflected away from beam direction by pressure built up between the colliding nuclei during the time of their mutual overlap. The affected particles quickly leave the interaction region where this transverse pressure acts. The directed flow has been reported to be highly sensitive towards various equations of state, in-medium nuclear effective

interactions [12] as well as towards entrance channel parameters such as combined mass [13], colliding geometries [14] as well as incident energy of projectile. Fig. 1.9 illustrates the preferential emission of the nucleons to positive scattering angles in the reaction plane giving rise to positive directed flow.

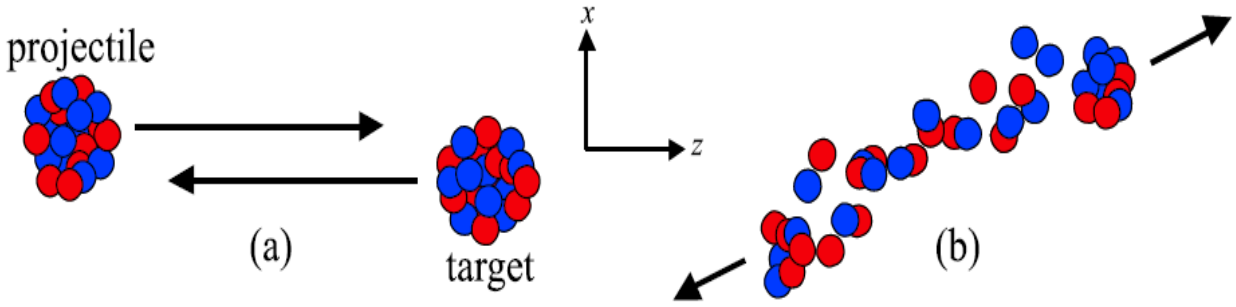

Fig 1.9: Schematic view of positive directed flow observed in non central collision.

The elliptic flow parameter $\langle v_1 \rangle$ is defined by:

$$\langle v_1 \rangle = \left\langle \frac{p_x}{p_t} \right\rangle$$

Where p_t is a transverse momentum defined as $p_t = \sqrt{p_x^2 + p_y^2}$, and p_x and p_y are projections of particle transverse momentum in perpendicular to reaction plane, respectively. There are several methods that are proposed in the literature to measure the directed flow. The transverse momentum method is widely used to analyze the directed flow over wide range of beam energies. The strength of the directed flow is measured by the slope of the transverse momentum of particles as a function of the rapidity.

$$F = \frac{d\langle p_x / A \rangle}{dY} | Y_{c.m.} = 0$$

Where $Y_{c.m}$. is rapidity in centre-of-mass frame. A more integrated quantity called "directed transverse momentum $\left\langle p_x^{dir} \right\rangle$" is also proposed to calculate the transverse momentum and is defined as [15]

$$\left\langle p_x^{dir} \right\rangle = \frac{1}{A} \sum_{i=1}^{A} sign\{Y(i) p_x(i)$$

Where Y(i) and $P_x(i)$ are, respectively, the rapidity and the momentum of i^{th} particle. Where rapidity of a particle is defined as

$$Y(j) = \frac{1}{2} \ln \frac{E(j) + p_z(j)}{E(j) - p_z(j)}$$

Where E(j) and $p_z(j)$ are, respectively, the energy and longitudinal momentum of j^{th} particle.

(c) Elliptical Flow

The name, elliptic flow, refers to the shapes of azimuthal distributions at midrapidity that resemble ellipses with major axis can be either in the reaction plane or out of the reaction plane and first introduced by H. Sorge in 1997 [11]. Here reaction plane is defined by the beam axis and a line joining the centres of the two colliding nuclei. The out of plane flow is also termed as squeeze out. The elliptic flow parameter $\langle v_2 \rangle$ is defined by:

$$\langle v_2 \rangle = \left\langle \frac{{p_x}^2 - {p_y}^2}{{p_x}^2 + {p_y}^2} \right\rangle$$

where p_x and p_y are the transverse components of the momentum. The positive value of $\langle v_2 \rangle$ represents in-plane elliptic flow and negative value represents squeeze out. A schematic view of in-plane and out of plane elliptic flow is shown in Fig. 1.10. Elliptical flow is expected to be larger in peripheral collisions.

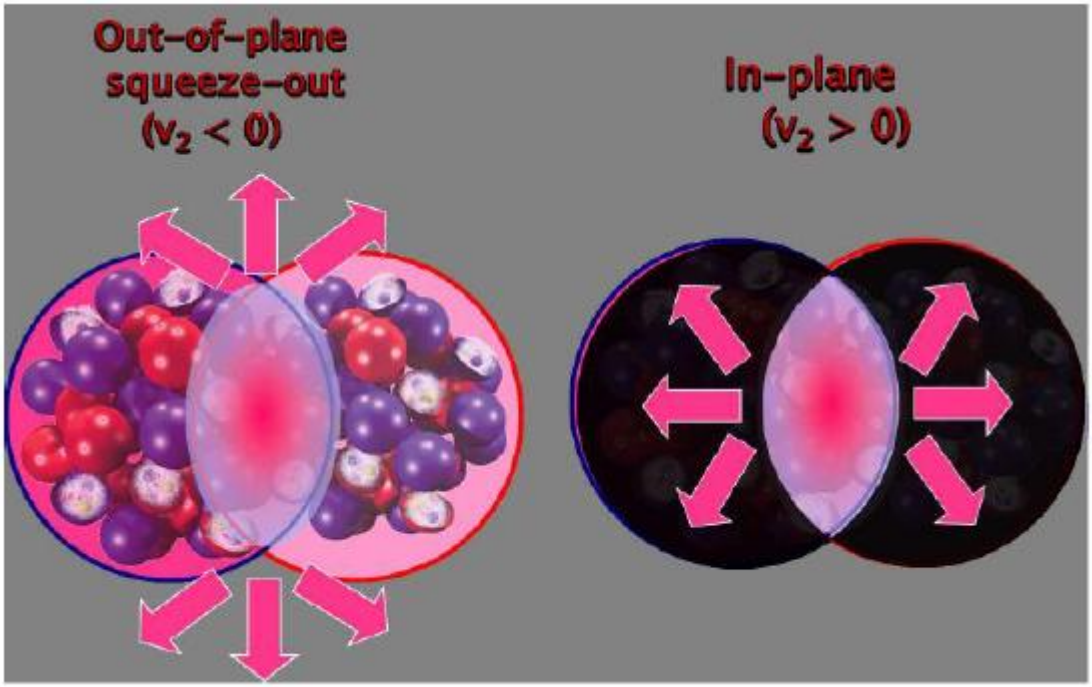

Fig. 1.10: In-plane and out-of-plane emission of the nucleons in the reaction plane (right side) and perpendicular to the reaction plane (left side), respectively.

1.7 Experimental efforts

The National Superconducting Cyclotron Laboratory (NSCL) at Michigan state University (MSU), USA firstly predicted the isospin effects in collective transverse flow for the reactions of ^{58}Fe+^{58}Fe and ^{58}Ni+ ^{58}Ni at incident energy of 55 MeV/nucleon and found that neutron-rich system exhibited larger flow (greater negative deflection) [16]. The energy of vanishing flow is also measured and neutron rich system is found to have higher energy of vanishing flow at all measured impact parameters.

The FOPI collaboration at GSI (Germany) also studied the reactions of ^{197}Au+^{197}Au and presented data on the directed flow for incident energies between 90 and 400 MeV/nucleon [17]. Similar study is also carried out by INDRA collaboration at GANIL (France) for the

reactions of ^{197}Au+^{197}Au at 40 and 150 MeV/nucleon and measured the directed and elliptic flows. Another study (by FOPI collaboration) has been done by Trautmann et al. [18] in which neutron and proton transverse flows are measured and found to be sensitive towards symmetry energy. Recently, FOPI collaboration also studied the central collisions of ^{40}Ca+^{40}Ca, ^{58}Ni+^{58}Ni, ^{96}Ru+^{96}Ru, ^{96}Zr+^{96}Zr, ^{129}Xe+CsI and ^{197}Au+^{197}Au at different incident energies ranging between 120 MeV/nucleon and 1.5 GeV/nucleon [19]. The transverse rapidity distribution and radial flow is measured for all the reactions.

The NIMROD-ISiS (Neutron Ion Multiplicity for Reaction Oriented Dynamics with Indiana Silicon investigation Sphere) collaboration at Texas A & M University (TAMU) in USA is also working actively in the field. The transverse flow of fragments for the reactions of ^{70}Zn+^{70}Zn, ^{64}Ni+^{64}Ni and ^{64}Zn+^{64}Zn at 35MeV/nucleon is measured by Kohley et al [20]. The measurements have shown that flow decreases with increase in the neutron content of fragment. Moreover, the effects of mass, charge and isospin-dependent components are also studied. The increased production of neutron-rich light charged particles (LCPs) in midrapidity region is also reported.

1.8 Theoretical Efforts

The isospin effects in transverse flow are predicted by Li *et al*. [21] by studying the reactions of ^{48}Ca+^{58}Fe and ^{48}Cr+^{58}Ni using Isospin-dependent Boltzmann-Uehling-Uhlenbeck (IBUU) model. The neutron-rich system is found to have stronger negative flow and proposed that isospin effects are due to the competition between various reaction mechanisms like symmetry energy, nucleon-nucleon cross section and Coulomb interactions. Similar results are also obtained by Chen *et al*. [22] using Isospin-dependent Quantum Molecular Dynamics (IQMD) model by measuring the flow for different fragments for the reactions of ^{58}Fe+^{58}Fe and ^{58}Ni+^{58}Ni at 55 MeV/nucleon and found that neutron-rich system has higher energy of vanishing flow. In addition to tansverse flow, isospin effects have been predicted in elliptic flow also. For example, the transverse and

elliptic flows for protons is studied for the reactions of $^{124}Sn+^{124}Sn$ at 50 MeV/nucleon using IBUU model and elliptic flow at transverse momenta is found to be sensitive towards the isospin dependence of equation of state [23]. Another study is also carried out by Di Toro et al. [24] for the reaction of $^{132}Sn+^{124}Sn$ at 1.5 GeV/nucleon and found that neutron-proton transverse and elliptic flow difference is sensitive to the symmetry energy. Recently, Gautam et al. [25] also studied the isospin effect on the balance energy by using the IQMD model, and also compared their findings with the other theoretical and experimental findings. Sood and Puri [26] have discussed the role of different cross sections on the balance energy (E_{bal}) throughout the mass range between 47 and 394. They found that largest cross section gives the more positive flow (hence smaller E_{bal}) followed by the second largest cross section. In another study Sood and Puri [27] studied the effect of momentum dependent interactions (MDI) on the collective flow as well as its disappearance throughout the mass range (from $^{12}C+^{12}C$ to $^{197}Au+^{197}Au$). They found that impact of MDI differs in lighter nuclei as compared to the heavier ones. S. Gautam and A. D. Sood [28] studied the effect of isospin degree of freedom on balance energy throughout the mass range between 50 and 350 for two sets of isobaric systems with N/A=0.54 and 0.57 as well as isobaric systems with N/A=0.5 and 0.58. They demonstrate clearly the dominance of Coulomb repulsion over symmetry energy. Gautam et al. [29] also studied the effect of isospin degree of freedom on the balance energy as a function of colliding geometry. So, in the present work, we aim to look, in details, the role of isospin momentum dependent interactions on directed transverse in-plane flow and its disappearance.

Chapter 2

Methodology

The study of intermediate heavy-ion collisions needs correct treatment of nuclear interactions. Naturally if projectile and target are of comparable size (symmetric) then reaction leads to high compression of the system whereas, asymmetric reactions lead to the heat or thermal energies. In collision dynamics reaction depends upon many parameters like energies of the projectiles their impact parameter and the mass of projectile and target. Time dependent Hartree Fock (TDHF) [30] Theory is used to describe the low energy heavy–ion collisions. It is used to study different physical processes with bombarding energies up to 10 MeV/nucleon where nucleon-nucleon collisions are negligible. For this purpose Extended TDHF (ETDHF) [31] is used. Intra nuclear cascade (INC) [32] model is capable of describing the high energy heavy ion collisions. This was the first microscopic dynamical model used to understand the experimental data of heavy ion collisions. In this model, the mean field is completely neglected and nucleon collisions are taken into account without Pauli blocking. Boltzmann-Uehling-Uhlenbeck (BUU) Model [33] includes nucleon-nucleon collisions with Pauli Blocking. BUU model is able to explain the one-body observables like collective flow, stopping and particle spectra. But event by event correlations cannot be analyzed within these models. IBUU model [34] is just like BUU model, in this model isospin dependence has been incorporated into the model by both the elementary nucleon-nucleon scattering cross section and the nuclear mean field. Quantum Molecular Dynamics (QMD) Model [35] is based on an event by event method. This simulation model has three steps:

- Initialization: to generate the nuclei.
- Propagation: to propagate nucleon under the influence of surrounding mean field.
- Collision: to collide nucleon if they come too close to each other.

QMD neglects the relativistic part and hence is valid for the incident energies below 1 GeV/nucleon. If one needs to go beyond this energy, one needs to take care of proper relativistic tools. Then we can use relativistic version of QMD i.e. RQMD. Also QMD does not include the isospin effects. Therefore modified version of QMD, i.e. IQMD has been developed. To carry out the present study we have used isospin dependent quantum molecular dynamics model.

2.1 Isospin Quantum Molecular Dynamics (IQMD) model

The Isospin Quantum Molecular Dynamics (IQMD) model [36] developed by Hartnack et al. is an extension of the QMD model which incorporates isospin degree of freedom. In Isospin Quantum Molecular Dynamics (IQMD) model the isospin degree of freedom enters through the cross-sections as well as in the Coulomb interactions. IQMD treats the different charge states of nucleons, deltas and pions explicitly. IQMD has been used for analysis of collective flow effects of nucleons and pions. In IQMD model neutron and proton are distinguish from each other. The isospin-dependent quantum molecular dynamics (IQMD) model treats different charge states of nucleons, deltas and pions explicitly, as inherited from the VUU model [37]. The IQMD model has been used successfully for the analysis of large number of observables from low to relativistic energies. This model also involve three important steps: First, one has to generate the nuclei. This procedure is called as initialization. Then propagate under the influence of surrounding mean field. This is termed as propagation. Finally, nucleons are bound to collide if they come too close to each other. This part is dubbed as collisions. The elastic and inelastic cross-sections for proton-proton, neutron-neutron as well as proton-neutron are supposed to be affected in the presence of isospin.

(a) Initialization

In this model the nucleons are represented by the Gaussian-shaped density distributions.

$$f_i(r,p,t) = \frac{1}{\pi^2\hbar^2} e^{-(r-r_i(t))^2 \frac{1}{2L}} e^{-(p-p_i(t))^2 \frac{2L}{\hbar^2}}$$

Here Gaussian width L is regarded as a description of the interaction range of a nucleon. The system dependence of L has been introduced in IQMD in order to obtain maximum stability of the nucleonic density profiles. For the heavier system (e.g. ^{197}Au + ^{197}Au), its value is chosen 8.66 fm^2, while for lighter one (i.e. ^{40}Ca + ^{40}Ca), the value is 4.33 fm^2.

Nucleons are initialized in a sphere with radius R = 1.12A$^{1/3}$ fm, in accordance with the liquid drop model. Each nucleon occupies a volume of h^3, so that phase space is uniformly filled. The initial momenta are randomly chosen between 0 and Fermi momentum (P_F), without any further local constraints. The Fermi momentum P_F depends on the ground state density. For ρ_0 = 0.17 fm^{-3}, it has a value of about 268 MeV/c. This possibility, however, gives a reduced binding energy per nucleon as compared to Weizsacker mass formula. Hence the initialized nuclei are less stable. On the other hand, this situation makes available the full Fermi-energy calculated from the Skyrme ansatz. The full Fermi pressure yields a stronger stability of the density profile against vibration modes. Moreover, the IQMD model performs a Lorentz contraction of the nucleus coordinate distribution, which becomes important at the higher energies. Fig. 2.1 shows the time evolution of the radii of ^{6}Li, ^{40}Ca, ^{131}Xe and ^{197}Au nuclei in coordinate space and the time evolution of Fermi momentum. The nuclei are found to be stable for a couple of hundred fm/c, which is long enough to study the reaction dynamics. It is found that heavier nuclei is more stable than a lighter nuclei. Once the target and projectile are generated with proper initialization, we boost them with proper center of mass velocity. In the following, we shall first discuss the propagation.

(b) Propagation

The successfully initialized nuclei are then boosted towards each other with proper centre of mass velocity using relativistic kinematics. Fig 2.2. shows the phase space distribution of Gold nucleus in X-Z and X-Y plane at incident energy 100 MeV/nucleon.

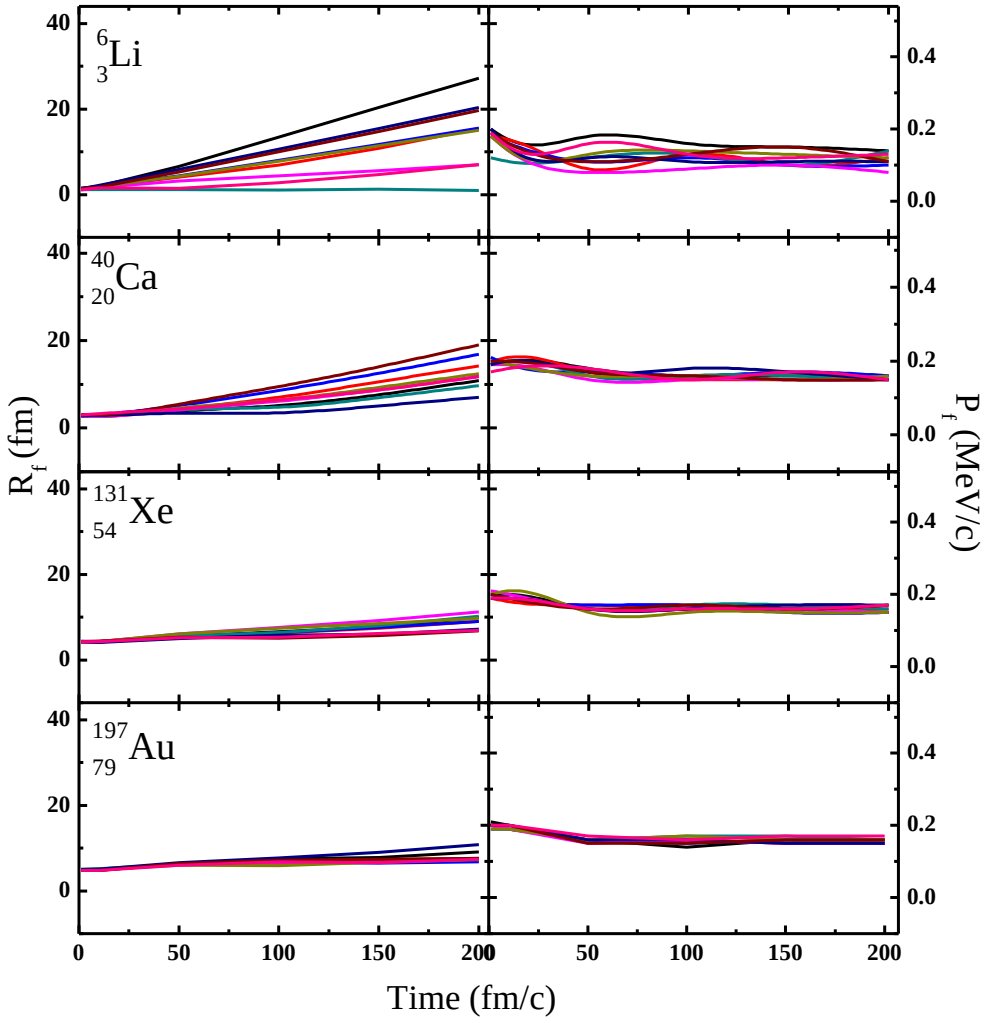

Fig. 2.1: Time evolution of radii and fermi momentum for ^{6}Li, ^{40}Ca, ^{131}Xe and ^{197}Au nuclei. Different lines correspond to number of events.

The panels from top to bottom are representing the positions at different times. The nucleons of target and projectile interact via two and three-body Skyrme forces, a Yukawa potential and momentum dependent interactions. The isospin degree of freedom is treated explicitly by employing symmetry potential and explicit Coulomb interactions among protons of colliding target and projectile. This helps in achieving correct distribution of protons and neutrons within nucleus. The hadrons propagate using Hamilton equations of motion:

$$\frac{dr_i}{dt} = \frac{\partial \langle H \rangle}{\partial p_i}; \qquad \frac{dp_i}{dt} = -\frac{\partial \langle H \rangle}{\partial r_i}$$

With

$$\begin{aligned} \langle H \rangle &= \langle T \rangle + \langle V \rangle \\ &= \sum_i \frac{p_i^2}{2m_i} + \sum_i \sum_{j>i} \int f_i(r, p, t) V^{ij}(r', r) \\ &\quad \times f_j(r', p', t) dr dr' dp dp'. \end{aligned}$$

The baryon-baryon potential V^{ij}, in the above relation, reads as:

$$V^{ij}(r'-r) = V^{ij}_{Skyrme} + V^{ij}_{Yukawa} + V^{ij}_{Coul} + V^{ij}_{mdi} + V^{ij}_{sym}$$

$$= \left(t_1 \delta(r'-r) + t_2 \delta(r'-r) \rho^{\gamma-1}\left(\frac{r'+r}{2}\right)\right) + t_3 \frac{\exp(|r'-r|/\mu}{(|r'-r|)/\mu} + \frac{Z_i Z_j e^2}{|r'-r|}$$

$$+ t_4 \ln^2 \left[t_5 (p_i' - p)^2 + 1 \right] \delta(r'-r) + t_6 \frac{1}{\rho_0} T_3^i T_3^j \delta(r_i' - r_j).$$

Here Z_i and Z_j denote the charges of i^{th} and j^{th} baryon, and T_3^i, T_3^j are their respective T_3 components (i.e. 1/2 for protons and -1/2 for neutrons). Meson potential consists of Coulomb interaction only. The parameters μ and t_1... t_6 are adjusted to the real part of the nucleonic optical potential. For the density dependence of nucleon optical potential, standard Skyrme-type parametrization is employed.

$$V_{loc} = \frac{\alpha}{2}\left(\frac{\rho}{\rho_0}\right) + \frac{\beta}{\gamma+1}\left(\frac{\rho}{\rho_0}\right)^2$$

Similar to the QMD, two different types of nuclear EOS have been implemented. A hard nuclear EOS with a compressibility of 380 MeV and a soft EOS wth a compressibility of 200 MeV [35]. The momentum dependence of NN interactions V^{MDI}, which may optionally be used in IQMD is fitted to experimental data on the real part of nucleon optical potential [38] which is yield:

$$V_{mdi} = \delta.\ln^2\left(\epsilon.(\Delta p)^2 + 1\right)\left(\frac{\rho}{\rho_0}\right)$$

The strength of symmetry energy is found to be equal to 32 MeV for normal nuclear matter density. Similarly, in the IQMD model the symmetry energy as a function of density becomes:

$$E_{sym}(\rho) = 32\left(\frac{\rho}{\rho_o}\right)^{\gamma} MeV$$

The term gamma (γ) determine the strength of symmetry at densities away from normal nuclear matter density. The role of momentum dependent interactions (MDI) in fragment production have been analyzed subjected to the different forms of density dependent symmetry energy. The term symmetry energy which accounts for for the isospin dependence of nuclear EOS also has an impact on the momentum depending interactions. A proper accounting of isospin dependence of momentum dependent interactions is required to extract the exact parametrization for the density dependence of symmetry energy.

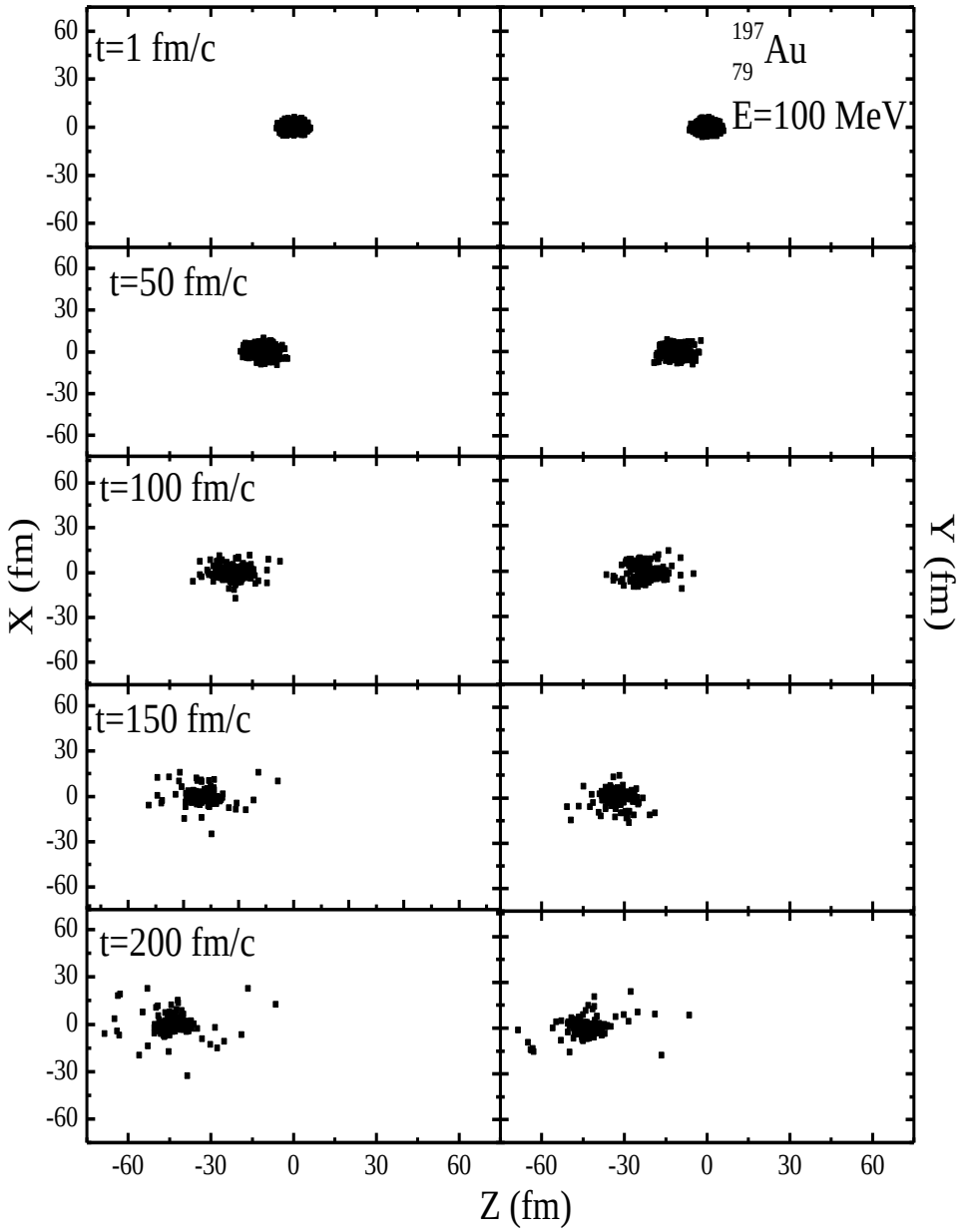

Fig. 2.2: Phase space distribution of nucleus in X-Z and X-Y plane. The Gold nucleus is initialized and propagated at energy 100 MeV/nucleon. The panels from top to bottom are representing the coordinate space of nucleons at different times.

(c) Collisions

The binary collisions are carried out stochastically, in a similar way as are done in all cascade models. During the propagation, two nucleons are supposed to suffer a binary collision if the distance between their centroids

$$\left|r_i - r_j\right| \le \sqrt{\frac{\sigma_{tot}}{\pi}}\ , \sigma_{tot} = \sigma\left(\sqrt{s}, type\right)$$

where "type" denotes the ingoing collision partners (N-N, N-Δ, N-π,...). In addition, Pauli blocking (of the final state) of baryons is taken into account by checking the phase space densities in the final states. The final phase space fractions P_1 and P_2 which are already occupied by other nucleons are determined for each of the scattering baryons. The collision is then blocked with probability

$$P_{block} = 1 - (1 - P_1)(1 - P_2).$$

Furthermore, parameterized free pn and pp cross-sections are used instead of averaged nucleon-nucleon cross-sections. The respective strength of different cross-sections is shown in Fig. 2.3. The total cross-section is the sum of the elastic and all inelastic cross-sections.

$$\sigma_{tot} = \sigma_{el} + \sigma_{inel} = \sigma_{el} + \Sigma_{channels}\sigma_i$$

The following inelastic reactions might influence the dynamics of the collision and are explicitly taken into account:

$NN \rightarrow \Delta N$ (hard-delta production) (a)

$\Delta \rightarrow N\pi$ (delta decay) (b)

$\Delta N \rightarrow NN$ (delta absorption) (c)

$N\pi \rightarrow \Delta$ (soft-delta production) (d)

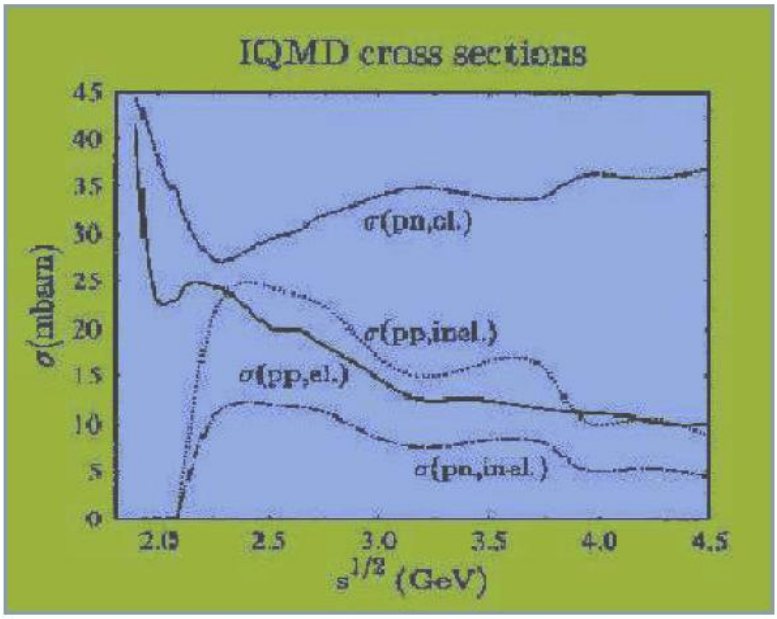

Fig. 2.3: The elastic and inelastic cross-sections for proton-proton (pp) and proton-neutron (nn) used in IQMD. The neutron-neutron (nn) cross-section is assumed to be equal to pp. The total cross-section is equal to sum of elastic and inelastic cross-section. Fig. is taken from ref. [36].

Elastic $\pi-\pi, \pi-\Delta, \Delta-\Delta, \Delta-N$ scattering is not taken into account. Experimental cross-sections are used for processes (a) and (d), as well as for the elastic N-N collisions. Inaccessible reactions like $\Delta N \to NN$ are calculated from their reverse reactions (here $NN \to \Delta N$) using modified detailed balance formula. The conventional detailed balance formula is only correct for particles with infinite lifetimes (zero width). The elastic nucleon-nucleon scattering angular distribution is taken to be

$$\frac{d\sigma_{el}}{d\Omega} \approx \exp\left[A(s)t\right]$$

Where t is $-q^2$, the transverse momentum transfer and

$$A(s) = 6\frac{[3.65(\sqrt{s}-1.8766)]^6}{1+[3.65(\sqrt{s}-1.8766)]^6}$$

$\sqrt{s}$ is the c.m energy in GeV and A is given in $(GeV/c)^{-2}$. The isospin degree of freedom play an important role especially for the particle production. The employed inelastic channels $NN \to NN^*$, $N\Delta$ and $\Delta\Delta$ are treated in an analogous fashion. In Fig. 2.4 phase space distributions of the projectile and target nucleons in X-Z and X-Y plane are shown. The reaction under study is ^{197}Au+^{197}Au at incident energy E=100 MeV/nucleon for central collisions. Similarly in Fig. 2.5 momentum space distribution of the projectile and target nucleons in P_x-P_z and P_x-P_y plane is shown.

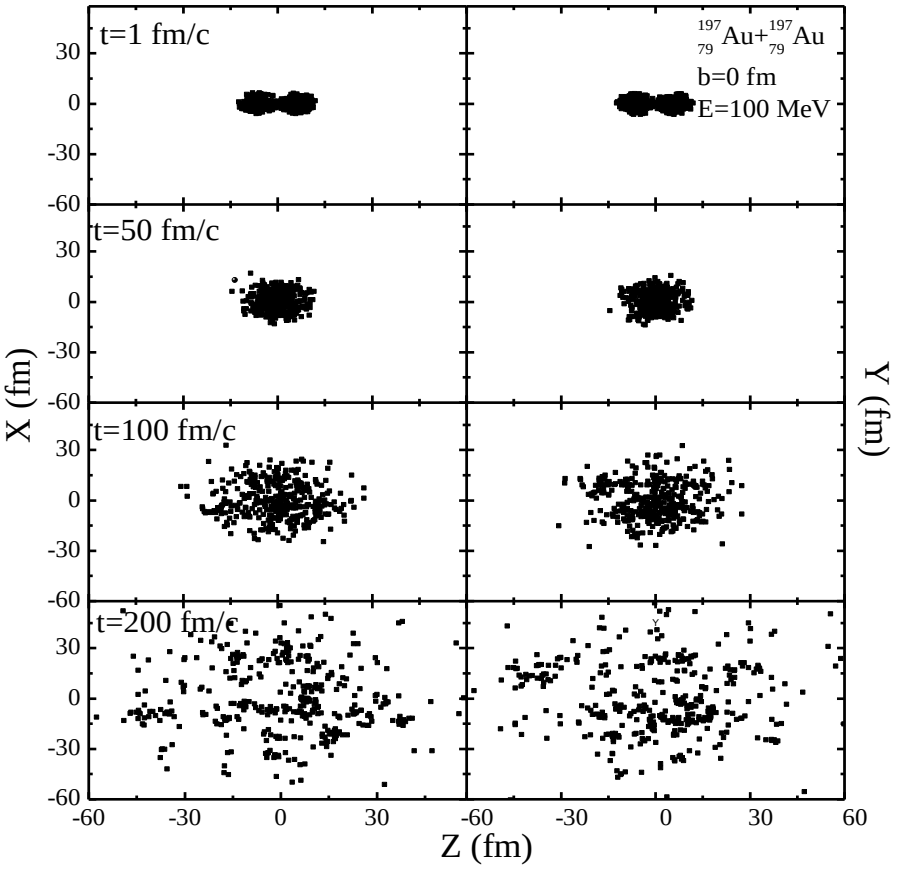

Fig. 2.4: Phase space distribution of the projectile and target nucleons in X-Z and X-Y plane. The reaction under study is ^{197}Au+^{197}Au at incident energy E=100 MeV/nucleon for central collisions. The panels from top to bottom are representing the coordinate space of nucleons at different times.

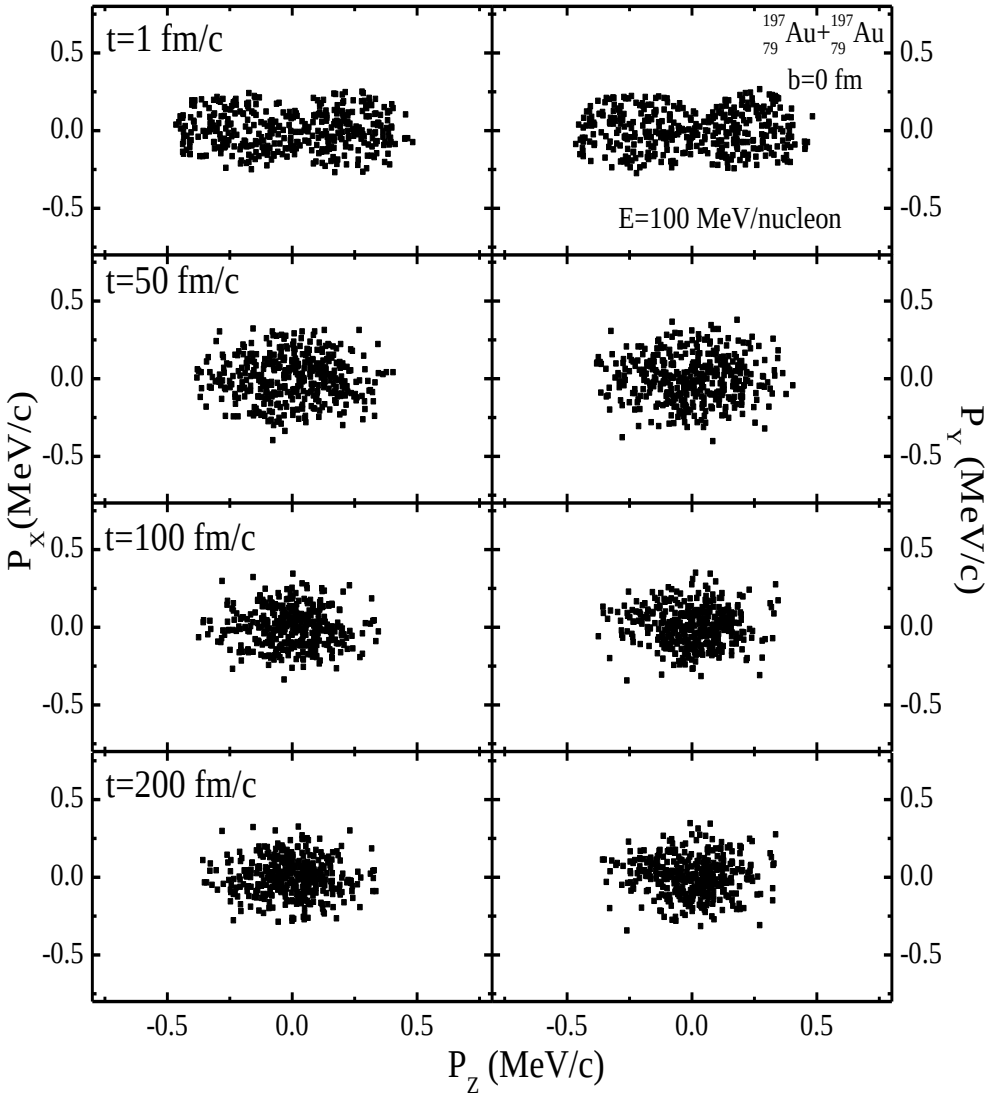

Fig. 2.5: Momentum space distribution of the projectile and target nucleons in P_x-P_z and P_x-P_y plane. The reaction under study is ^{197}Au+^{197}Au at incident energy E=100 MeV/nucleon for central collisions. The panels from top to bottom are representing the positions at different times.

In Fig. 2.6 we display the time evolution of collision rate for different soft equation of states with momentum dependent interactions (SMD) without momentum dependent interactions (Soft EOS) and with isospin dependence of SMD (Iso-SMD). The number of collisions is suppressed in case of MDI interactions and in case of isospin dependence of MDI interactions. MDI interactions are repulsive in nature, when matter is highly compressed, the nucleon-nucleon correlations are already broken due to violent nucleon-nucleon collisions. As a result, fewer collisions take place.

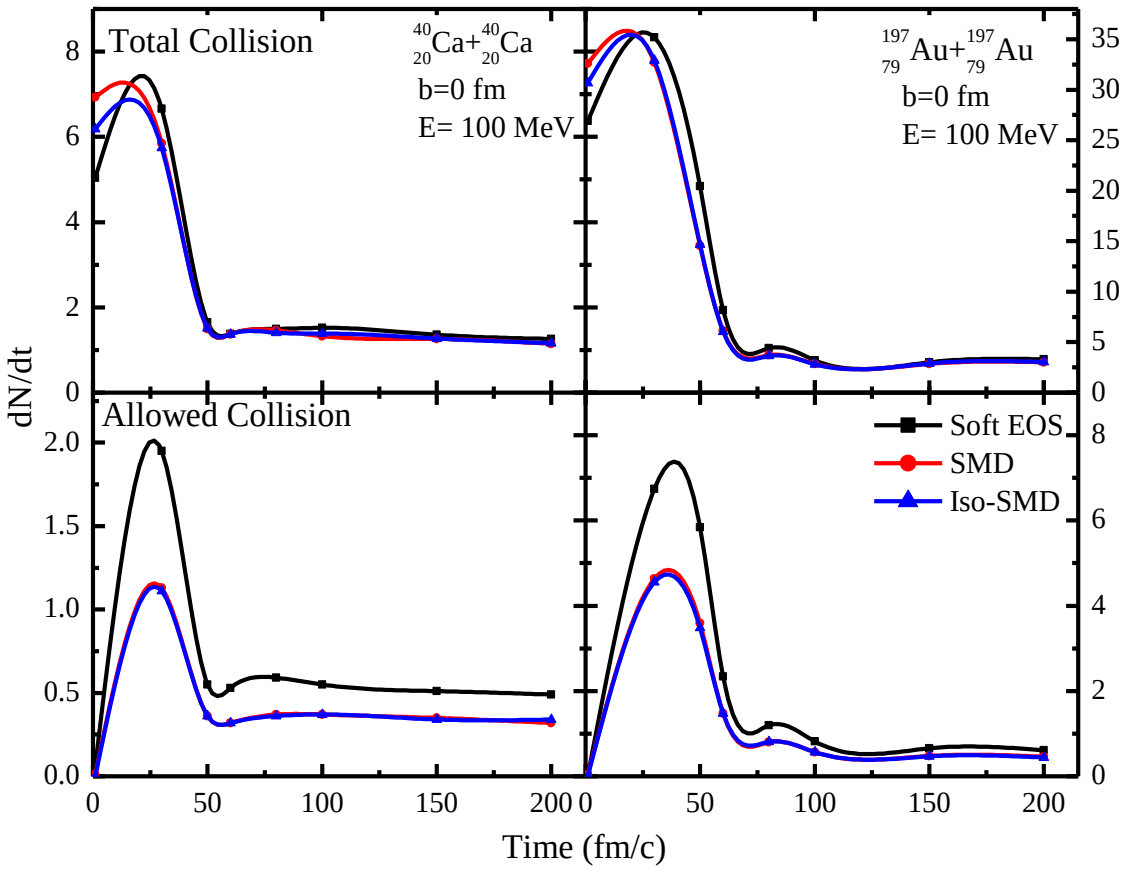

Fig. 2.6: Graph shows the time evolution of collision rate for different soft equation of states with momentum dependent interactions (SMD) without momentum dependent interactions (Soft EOS) and with isospin dependence of SMD (Iso-SMD).

Chapter 3

Influence of Isospin Momentum Dependent Interactions on Directed Transverse Flow

3.1 Disappearance of Directed Transverse Flow: Energy of Vanishing Flow

The directed flow results from the combined effects of the attractive mean field and nucleon-nucleon scattering governed by the in-medium nucleon-nucleon (*NN*) cross section. The outcome of a reaction may lead to either positive or negative flow depending on the incident energy of the reaction. At low incident energies, mean field dominate the reaction dynamics, therefore leading to a negative directed flow. On the other hand, as the incident energy increases, nucleon-nucleon scattering becomes important and nucleons are scattered to positive scattering angles, leading to positive directed flow. When both the attractive and repulsive interactions counterbalance each other at particular incident energy, net flow disappears. The incident energy at which flow disappears is often known as the Balance energy or energy of vanishing flow.

A schematic representation of the directed transverse flow in the centre of mass frame for three incident energies: (a) $E<E_{bal}$; (b) $E=E_{bal}$; and (c) $E>E_{bal}$ is shown in fig. 3.1. In this diagram the projectile P moves from left to right along the z-axis, and collides with the target T moving in the opposite direction (the x-y plane is perpendicular to the beam direction).

1. For $E< E_{bal}$ where the interaction is dominated by the attractive mean field, the particles are mainly scattered away from the projectile side of the reaction plane (to negative angles).

2. For $E>E_{bal}$ where the interaction is dominated by the repulsive nucleon-nucleon scattering, the particles are mainly scattered toward the projectile side of the reaction plane(to positive angles).
3. For E=Ebal these two effects balance, the particles are symmetrically deflected in the reaction plane, and the directed transverse flow vanishes.

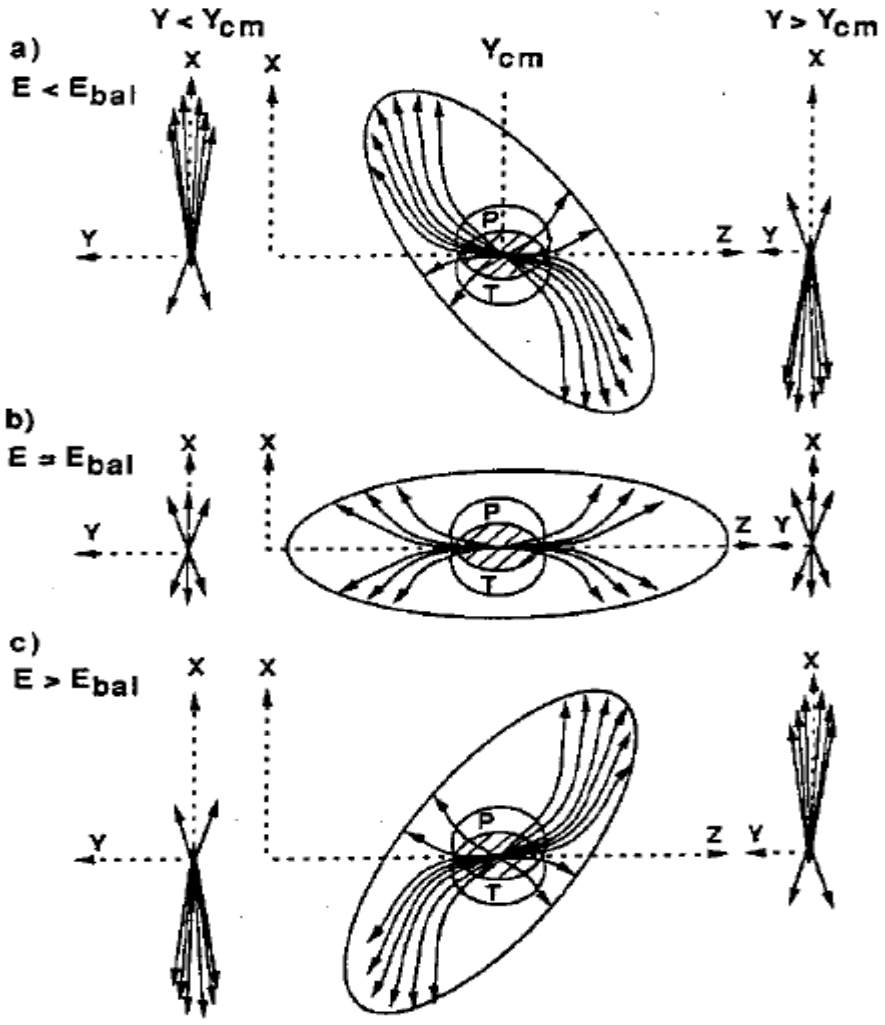

Fig. 3.1: Diagrammatic representation of the forward and backward flow side of the reaction plane for three incident energies: (a) $E<E_{bal}$ (b) $E=E_{bal}$ (c) $E>E_{bal}$.

3.2 Momentum Dependent Interactions

The knowledge of the nuclear compressibility is not only relevant for the nuclear physics, but also vital for other branches such as astrophysics. As earlier explained the compressibility depends not only on the density but also the entire momentum plane. In other words, equation of state apart from the population of nucleons also depends upon their relative velocities. This can also seen from the optical potential where strong momentum dependence was reported in the literature. The momentum dependent interaction (MDI) obtained by parametrizing the momentum dependence of the real part of the optical potential.

$$V^{MDI} = t_4 \ln^2 (t_5 (p_1-p_2)^2+1) (r_1-r_2)$$

With parameters t_4=1.57 MeV and $t_5=5\times10^{-4}$ MeV^{-2}. For the momentum dependent interactions, which may optionally be used in QMD/IQMD, is fitted to experimental data on the real part of the nucleon optical potential , which yields:

$$V_{mdi} = \delta.\ln^2\left(\in.(\Delta p)^2 + 1\right)\left(\frac{\rho}{\rho_0}\right)$$

These momentum dependent interactions, give rise to two new equations of state. A set with momentum dependent interactions and soft equation of state is called SMD, whereas a hard equation of state with momentum dependence interactions is called HMD. The equation of state (EOS) in its standard Skyrme-type parameterization including momentum dependence then reads:

$$U = \alpha\left(\frac{\rho}{\rho_0}\right) + \beta\left(\frac{\rho}{\rho_0}\right)^{\gamma} + \delta.\ln^2\left(\in.(\Delta\vec{p})^2 + 1\right)\left(\frac{\rho}{\rho_0}\right)$$

The parameters t_1....t_5 are uniquely related to the corresponding values of α, β, γ, $\delta.\in$. The values of these parameters corresponding to new analysis of Hama et al. [39] are shown in the table 3.1.

K (MeV)	α (MeV)	β (MeV)	ɣ	δ (MeV)	$\in$	EOS
200	-356	303	1.17	-	-	S
380	124	70.5	2	-	-	H
200	-390(-3189)	320(3176)	1.14(1.011)	1.57	21.54	SMD
380	-130(-63.13)	59(49.42)	2.09(2.12)	1.57	21.54	HMD

Table 3.1. Parameters of static and momentum dependent potentials.

The momentum dependence of the equation of state has attracted a lot of considerations. If matter is highly compressed, the nucleon-nucleon correlations are already broken due to violent nucleon-nucleon collisions. The momentum dependence of the nuclear equation of state has been reported to affect the collective flow and particle production drastically. During the initial phase of the collision (when two nuclei with large relative momentum penetrate each other), effect of the MDI is very strong. The particles propagating with momentum dependent interactions are accelerated in the transverse direction during early phase of the reaction. As a result, fewer collisions take place and the transverse flow increases considerably. The pion yield was found to be suppressed by 30% once momentum dependent interactions were included in the evolution of reaction. MDI's also suppressed the nucleon-nucleon collisions by the same amount. The momentum dependent interactions are also found to affect the multifragmentation and nuclear stopping. So momentum dependent interactions play an important role in heavy ion collisions at intermediate energies.

As discussed earlier, the momentum dependence of mean field potential has a crucial role to play in the description of heavy-ion collisions. The individual momentum of the particle has a negligible role until the projectile and target nuclei overlap with each other. As soon as the projectile and target begin to overlap (see Fig.3.2 [a]), the interaction takes

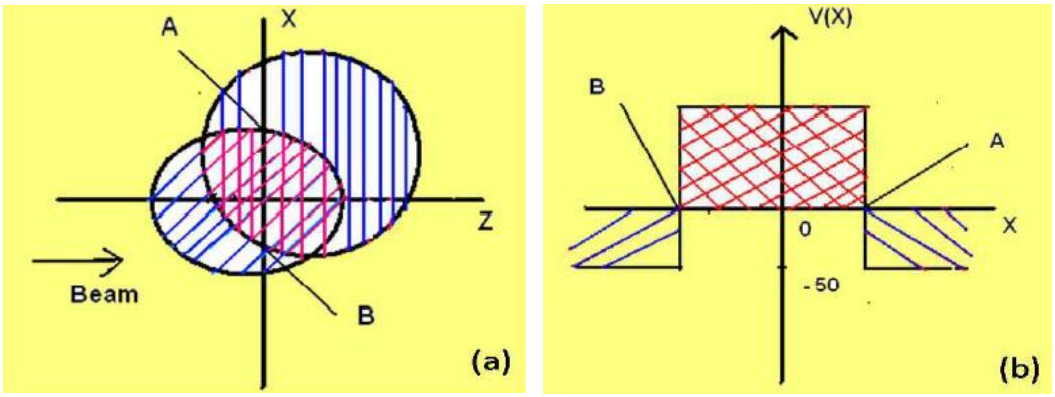

Figure 3.2: Transverse momentum caused by momentum dependent forces. (a) The reaction in the beam-impact parameter plane. (b) Graphical view of the potential produced in the reaction. We see in the overlap region strong repulsive and outside it an attractive potential.

place between the nucleons of projectile and target, which has a large relative momentum. Due to such a large relative momentum, the projectile nucleons feel a strong repulsion due to target nucleons in the overlap region and vice versa (see Fig.3.2[b]), while the nucleons in the spectator zone are either from the target or projectile, and hence potential is still attractive in that region(see Fig.3.2[b]). This deflects the nucleons in transverse direction during early phase of the reaction, resulting in the transfer of the momentum in the radial direction. This can result in decrease in density as well as number of collisions. We see that the no difference is observed in the soft, hard, SMD and HMD equations of state at normal nuclear matter density. On the other hand, the difference between different equations of state goes on increasing with increase in density above normal nuclear matter density. This motivated us to perform the study with momentum dependent interactions in intermediate energy heavy-ion collisions. If we introduced isospin degree of freedom into the momentum-dependent interaction and obtain an isospin momentum dependent interaction it becomes more interested.

3.3 Isospin Momentum Dependent Interactions

Although the role of MDI on the dynamical process in the heavy ion collisions has been in usage for many years, the isospin effect of the MDI has never been taken into account. Recently, Liu et al. [40] considered an isospin degree of freedom in MDI to obtain isospin momentum dependent interactions (Iso-MDI). To study the role of Iso-MDI on the isospin fractionation ratio and its dynamical mechanism in the intermediate energy heavy ion collisions, they insert an isospin degree of freedom into the MDI in IQMD to obtain the Iso-MDI for simulation in IQMD. It is found that the Iso-MDI brings an important isospin effect into the isospin fractionation ratio. It is found that the Iso-MDI reduces obviously the reduction of isospin fractionation ratio. Thus the isospin dependence of momentum-dependent interaction is thus important for studying accurately the equation of state of isospin asymmetry nuclear matter. For further investigation of the density dependence of symmetry energy we included the isospin momentum dependent interactions in IQMD model. The methodology was based on the fact that neutron-proton correlation is stronger than neutron-neutron or proton-proton correlation [41]. We introduced the momentum-dependent interactions as a function of isospin term $V^{\text{Iso-MDI}}$ in IQMD model as:

$$V^{Iso-MDI} = \left(1.0 - 0.5 T_{3i} T_{3j}\right) V^{MDI}$$

Where T_{3i}, T_{3j} are the isospin components of interacting baryons and this new model with Iso-MDI is known as IQMD (TU01).

3.4 Results and discussion

For the present analysis, we simulate several thousands of events of each reaction at incident energies around E_{bal} in small steps of 10 MeV/nucleon for each isotopic system of Ca+Ca and Xe+Xe. In particular, we simulate the reactions $^{40}Ca+^{40}Ca$, $^{44}Ca+^{44}Ca$, $^{52}Ca+^{52}Ca$, $^{56}Ca+^{56}Ca$, $^{60}Ca+^{60}Ca$ for colliding geometry ($b/b_{max}=0.4$) and $^{120}Xe+^{120}Xe$, $^{124}Xe+^{124}Xe$, $^{130}Xe+^{130}Xe$, $^{136}Xe+^{136}Xe$, $^{140}Xe+^{140}Xe$ for colliding geometry (b=0-3 fm).

Such systematic studies performed at intermediate incident energies IQMD model. We used soft equation of state (EOS) and hard EOS with and without MDI, labeled respectively, Soft, SMD and Hard, HMD. And also introduced isospin degree of freedom in MDI interaction in IQMD model as explained earlier so two more EOS are used i.e. soft Iso-MDI and hard Iso-MDI, which are labled as Iso-SMD and Iso-HMD.

3.4.1 Transverse momentum dependence of Transverse flow at different impact parameters

The directed, elliptic, triangular and higher order anisotropic flows can measured from the azimuthal distributions of the particles as:

$$\frac{dN}{d\phi} = a_0\left[1 + a_1\cos\phi + a_2\cos 2\phi + a_3\cos 3\phi + a_4\cos 4\phi ...\right].$$

Here, ϕ is the azimuthal angle between the transverse momentum of the particle and reaction plane. The coefficients a_1 and a_2 correspond to the strength of the directed and elliptic flow contributions, respectively, $\langle v_1 \rangle$ can be related to Fourier coefficient a_1 by recognizing that

$$\langle v_1 \rangle = \left\langle \frac{p_x}{p_t} \right\rangle = \langle \cos(\phi) \rangle$$

Where p_t is a transverse momentum defined as $p_t = \sqrt{p_x^2 + p_y^2}$, and p_x and p_y are projections of particle transverse momentum in perpendicular to reaction plane, respectively. $\langle v_1 \rangle$ is also called as directed flow parameter. It is the measure of the collective motion of the particles in the reaction plane.

To study the effect of MDI and Iso-MDI on transverse flow as a function of transverse momentum in Fig. 3.3 and Fig. 3.4, we display the directed flow $\langle v_1 \rangle$ as a function of transverse momentum (p_t) at different impact parameter ranges e.g. $\hat{b}$ =0.0-0.4, $\hat{b}$ =0.4-0.6

and $\hat{b}$ =0.6-0.8 for ^{40}Ca+^{40}Ca and ^{124}Xe+^{124}Xe for different EOS at energy 400 MeV/nucleon. In Fig. 3.3 black, red and blue lines are for Soft, SMD and Iso-SMD EOS and in Fig. 3.4 violet, orange, green lines are for Hard, HMD and Iso-HMD EOS. With the inclusion of MDI and Iso-MDI results in larger positive value of $\langle v_1 \rangle$ for projectile-like region and larger negative value for target-like region. This is due to the repulsive nature of MDI. There is also a reduction of $\langle v_1 \rangle$ for Iso-MDI interactions from MDI but only at higher impact parameters. This happens because when isospin degree of freedom is introduced in MDI the neutron-proton cross section is three times larger than the neutron-neutron and proton-proton cross section that will effect binary collisions. This effect is same for both soft EOS and hard EOS. This shows a dependence of directed flow on symmetry potential. For smaller size system affect of MDI and Iso-MDI is large as compared to larger system and for larger mass system the value of directed flow is maximum and minimum for lighter mass system.

3.4.2 Transverse flow as a function of rapidity at different impact parameters

Transverse flow has great dependence on rapidity. The rapidity is defined as, $Y^{red} = Y_{c.m.} / Y_{beam}$, and $Y_{c.m.}$ is given by:

$$Y_{c.m.} = \frac{1}{2} \ln \frac{E(i) + p_z(i)}{E(i) - p_z(i)},$$

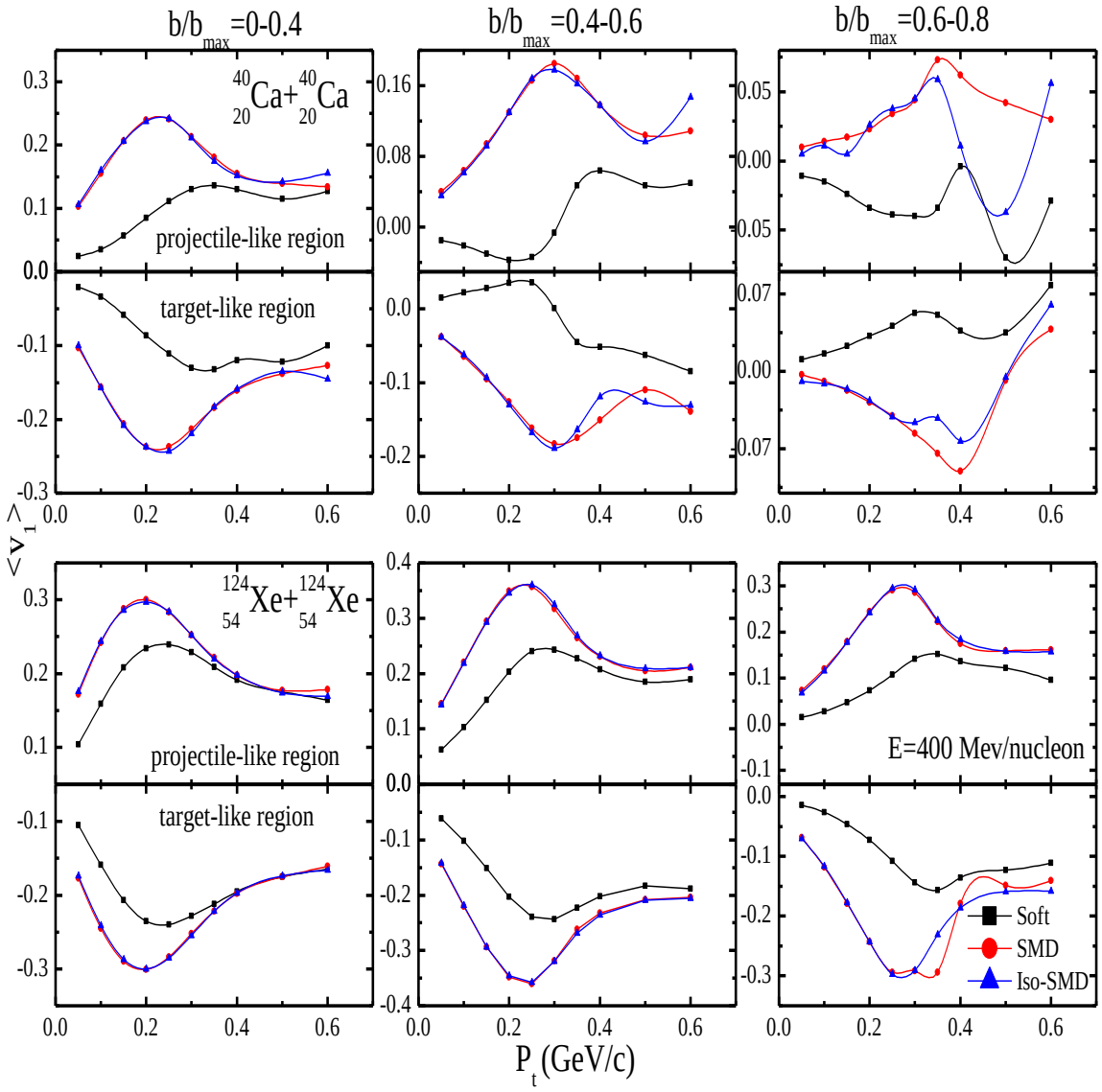

Fig. 3.3: Transverse flow $\langle v_1 \rangle$ as a function of transverse momentum (p_t) for soft EOS at different impact parameters $\hat{b}$ =0.0-0.4, $\hat{b}$ =0.4-0.6 and $\hat{b}$ =0.6-0.8. Upper panel is for ^{40}Ca+^{40}Ca and lower panel is for ^{124}Xe+^{124}Xe at energy 400 MeV/nucleon. Black, red and blue lines are for Soft, SMD and Iso-SMD EOS.

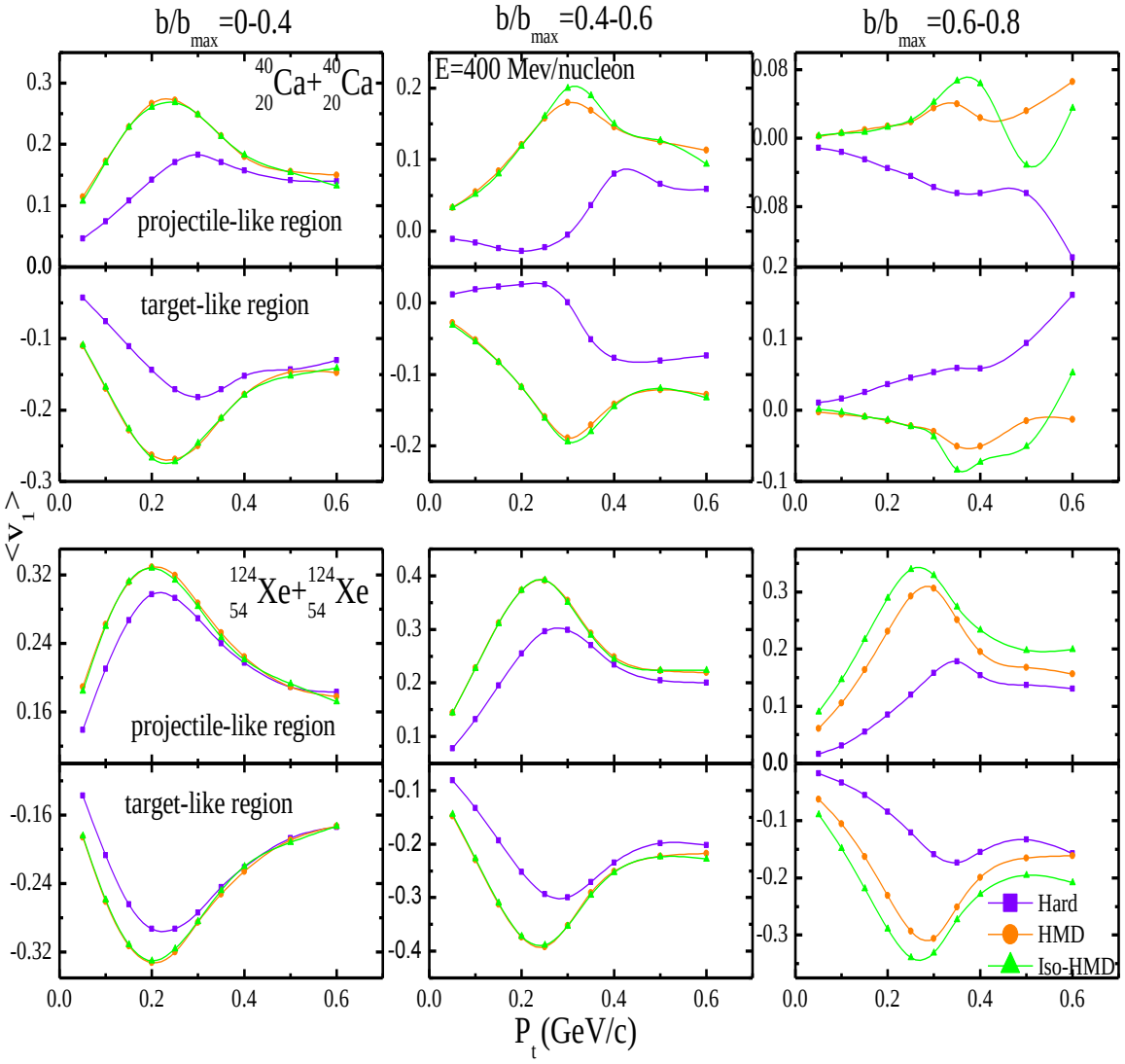

Fig. 3.4: Transverse flow $\langle v_1 \rangle$ as a function of transverse momentum (p_t) for hard EOS at different impact parameters $\hat{b}$ =0.0-0.4, $\hat{b}$ =0.4-0.6 and $\hat{b}$ =0.6-0.8. Upper panel is for ^{40}Ca+^{40}Ca and lower panel is for ^{124}Xe+^{124}Xe at energy 400 MeV/nucleon. Violet, orange, green lines are for Hard, HMD and Iso-HMD EOS.

Where, E(i) and $p_z(i)$ are the energy and longitudinal momentum of the ith particle, respectively. $\langle v_1 \rangle$ as well as to excitation function of reduced flow $\left(\frac{\partial v_1}{\partial y}\Big|_{midr} \right)$ at intermediate energies can give better idea about balance energy. For this purpose we simulate the reactions at incident energy 400 MeV/nucleon for ten thousand events. In particular, we simulate the reactions ^{40}Ca+^{40}Ca and ^{124}Xe+^{124}Xe at different impact parameter ranges e.g. $\hat{b}$ =0.0-0.4, $\hat{b}$ =0.4-0.6 and $\hat{b}$ =0.6-0.8 at energy 400 MeV/nucleon. In fig. 3.5, we display $\langle v_1 \rangle$ as a function of rapidity at different impact parameters for different equation of states. Solid black, red and blue lines are for soft, SMD and Iso-SMD equation of states and similarly violet, orange and green solid lines are for hard, HMD and Iso-HMD equation of states. We found that the role of MDI and Iso-MDI is larger for larger colliding geometries as compared to smaller colliding geometries. For imapact parameter $\hat{b}$ =0.6-0.8 there is a large reduction in flow. For lower mass system the effect of MDI and IMDI is large as compared to larger system.

In Fig. 3.6 and 3.7 we display the $\langle v_1 \rangle$ as a function of rapidity for neutrons and protons at different impact parameters for different EOS. Fig. 3.6 is for soft EOS and Fig.3.7 for hard EOS. Different lines have same meaning as in Fig. 3.5. The maximum value of $\langle v_1 \rangle$ is larger for protons as compared to neutrons. For heavy mass system $\langle v_1 \rangle$ is large and small of smaller mass system. Similarly, the affect of MDI and Iso-MDI is larger at higher colliding geometries as compared to smaller ones.

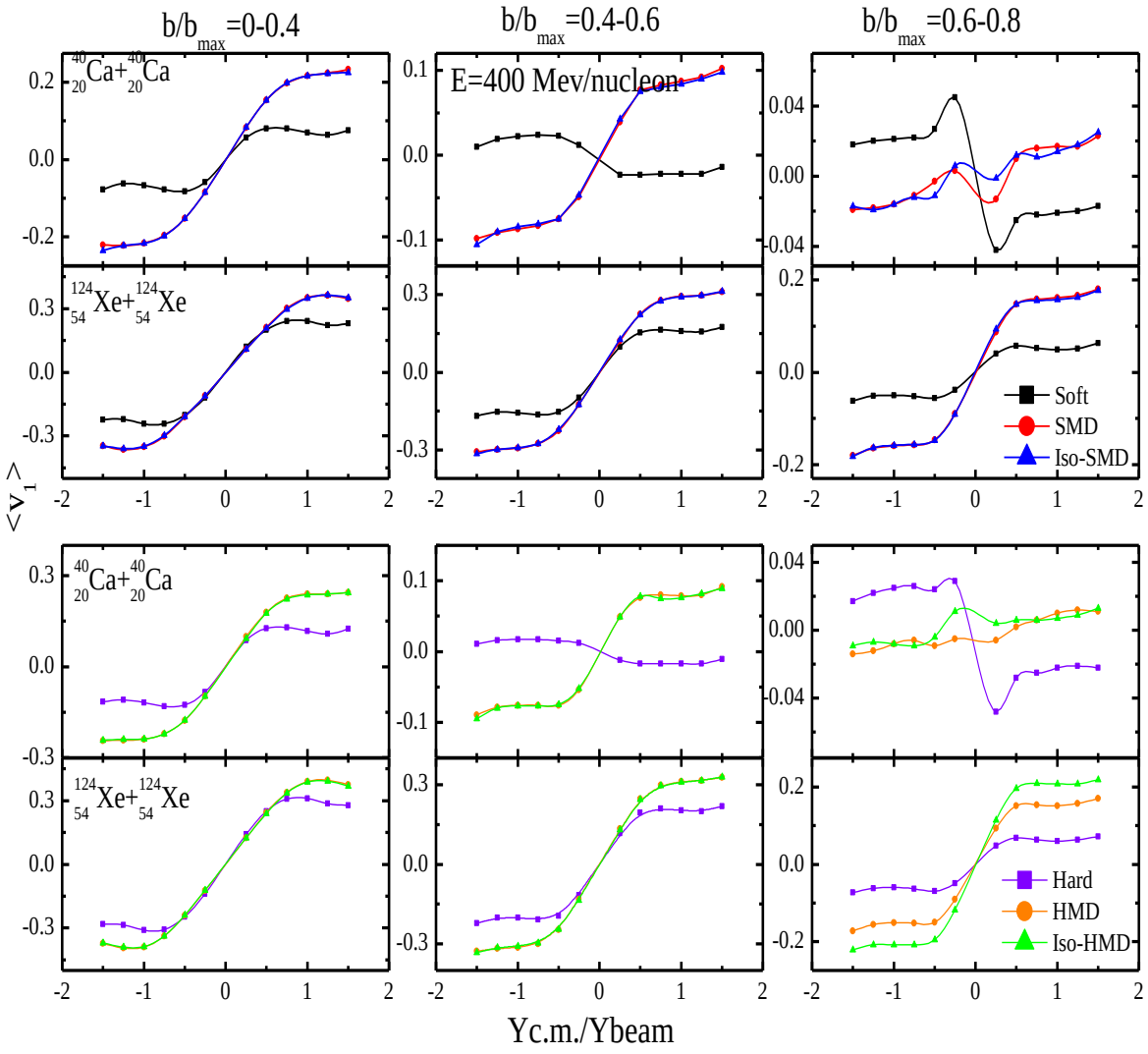

Fig. 3.5: $\langle v_1 \rangle$ as a function of rapidity at different impact parameters $\hat{b}$ =0.0-0.4, $\hat{b}$ =0.4-0.6 and $\hat{b}$ =0.6-0.8. Upper panel is for soft EOS and lower panel is for hard EOS. Different lines are explained in text.

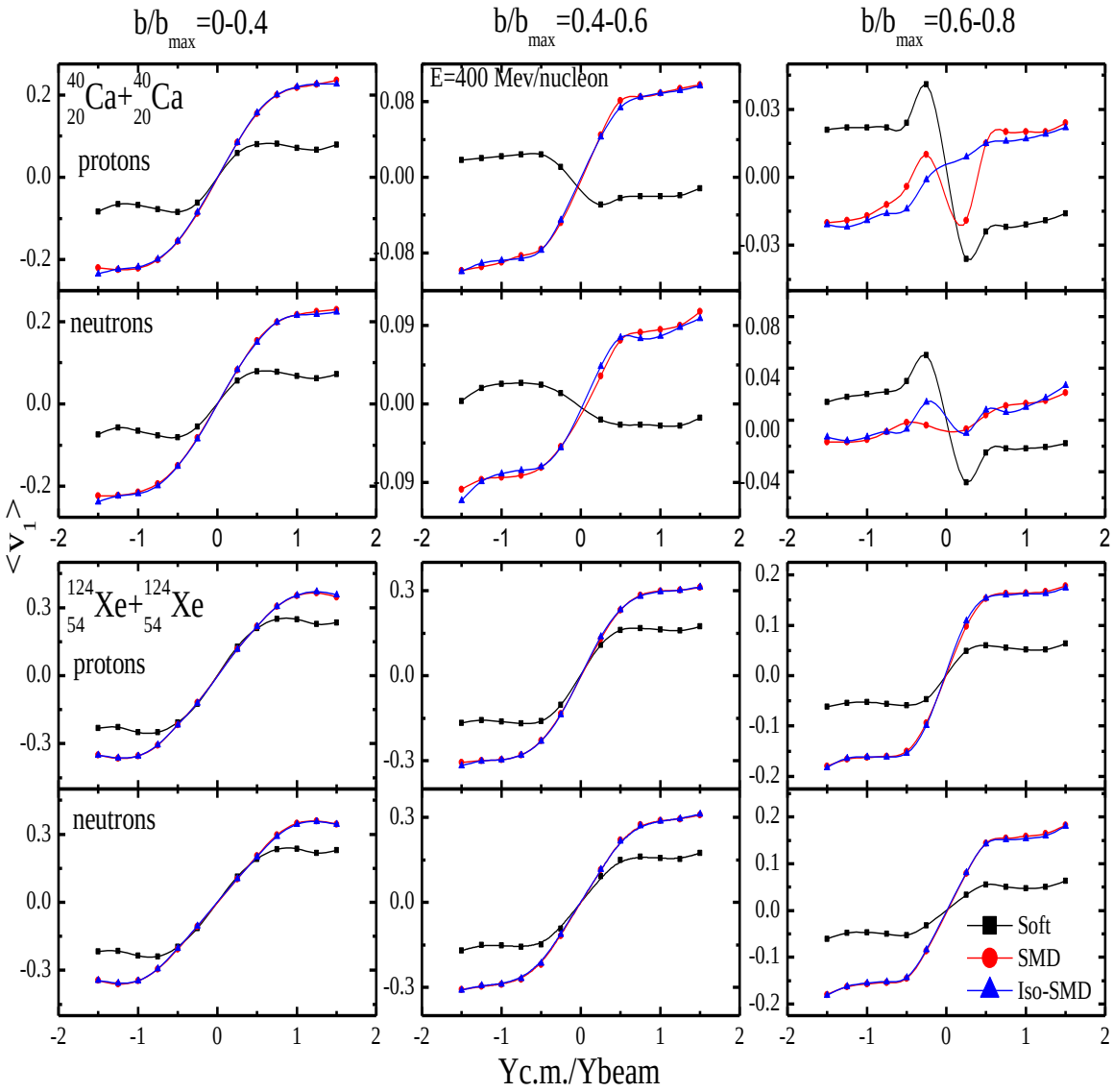

Fig. 3.6: $\langle v_1 \rangle$ as a function of rapidity for protons and neutrons at different impact parameters $\hat{b}$ =0.0-0.4, $\hat{b}$ =0.4-0.6 and $\hat{b}$ =0.6-0.8 for soft EOS. Upper panel is for ^{40}Ca+^{40}Ca and lower panel is for ^{124}Xe+^{124}Xe. Different lines are explained in text.

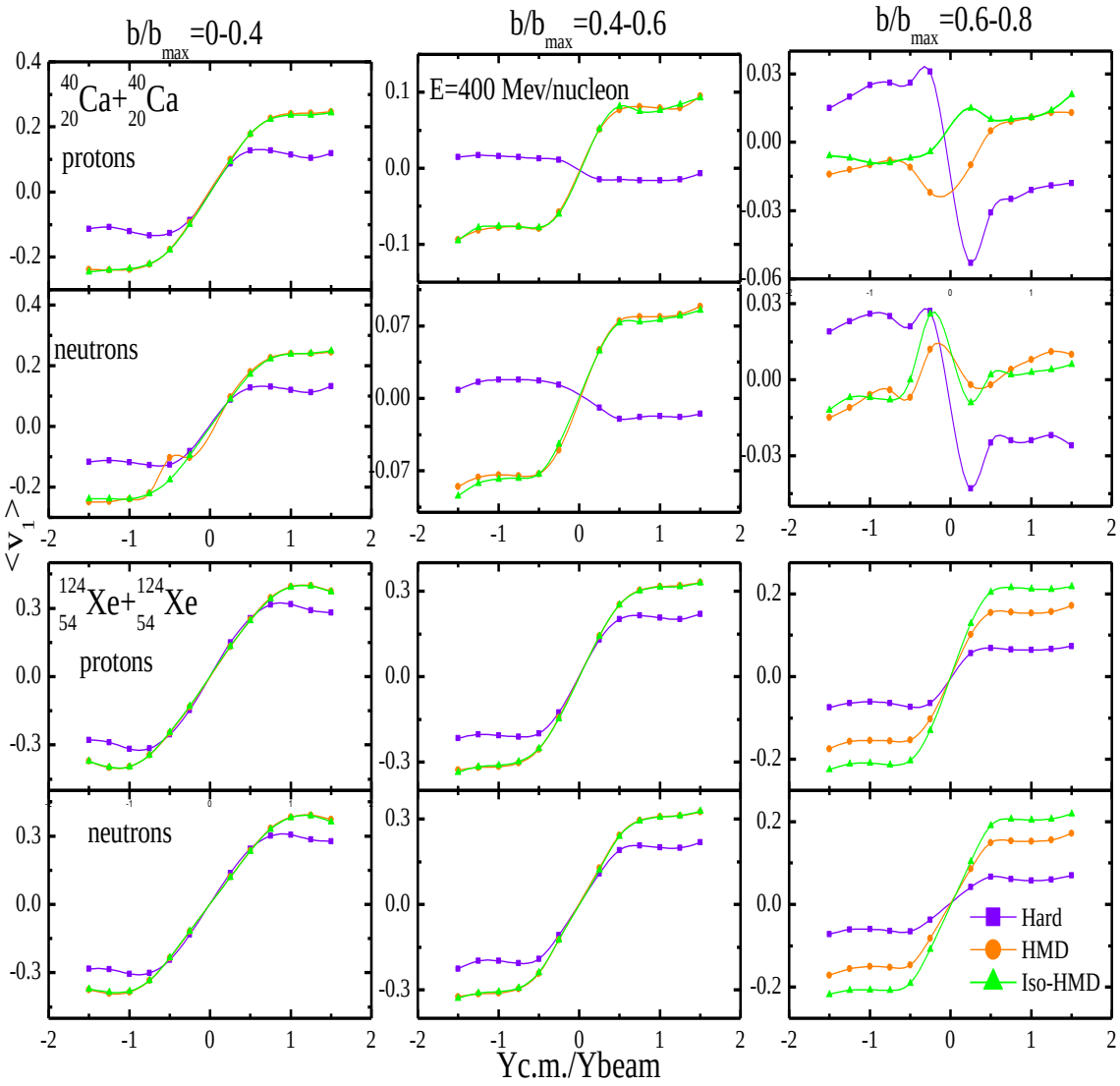

Fig. 3.7: $\langle v_1 \rangle$ as a function of rapidity for protons and neutrons at different impact parameters $\hat{b}$ =0.0-0.4, $\hat{b}$ =0.4-0.6 and $\hat{b}$ =0.6-0.8 for hard EOS. Upper panel is for ^{40}Ca+^{40}Ca and lower panel is for ^{124}Xe+^{124}Xe. Different lines are explained in text.

3.4.3 Time evolution of directed Transverse flow

There are several methods in the literature to define the nuclear transverse in-plane flow. In the most of studies, the EVF is extracted from $\langle p_x / A \rangle$ plots where one plots $\langle p_x / A \rangle$ as a function of reduced rapidity $Y_{c.m.} / Y_{beam}$. Using a linear fit to the slope, one can find the so-called reduced flow F. Naturally, the energy at which the reduced flow passes through zero is called the EVF. Alternatively, one can also use more integrated quantity "directed transverse momentum $\langle p_x^{dir} \rangle$". However $\langle p_x^{dir} \rangle$ presents an easier way to measure the in-plane flow rather than complicated functions such as $\langle p_x / A \rangle$ plots. It has been shown in [28] that the disappearance of flow occurs at the same incident energy in both the cases showing the equivalence between $\langle p_x / A \rangle$ plots and $\langle p_x^{dir} \rangle$ as far as the EVF is concerned. In Fig. 3.8, we display the time evolution of the $\langle p_x^{dir} \rangle$ for ^{40}Ca+^{40}Ca (left panels) and ^{124}Xe+^{124}Xe (right panels) at colliding geometry (b/b_{max}=0.4) at energy 100 MeV/nucleon. The solid black, red and blue lines represent $\langle p_x^{dir} \rangle$ for soft, SMD and Iso-SMD equation of states and similarly violet, orange and green solid lines represent $\langle p_x^{dir} \rangle$ for hard, HMD and hard Iso-HMD equation of states. From the figure, we see that the $\langle p_x^{dir} \rangle$ is negative at the start of reaction because of the dominance of attractive mean field interactions during the initial phase of the reaction. These interactions remain attractive or may turn repulsive depending on the incident energies. The $\langle p_x^{dir} \rangle$ remains negative for the lower incident energies but turns positive at higher beam energies. At higher energy the repulsion due to momentum-dependent interactions is stronger during the early phase of the reaction and transverse momentum increases sharply. Iso-MDI induces the reduction of $\langle p_x^{dir} \rangle$ from both SMD and HMD equation of state as shown in Fig. 3.3. However, the overall effect depends on the mass of the colliding nuclei. Note that the lighter colliding nuclei show a huge variation for all equation of states compared to the heavy ones.

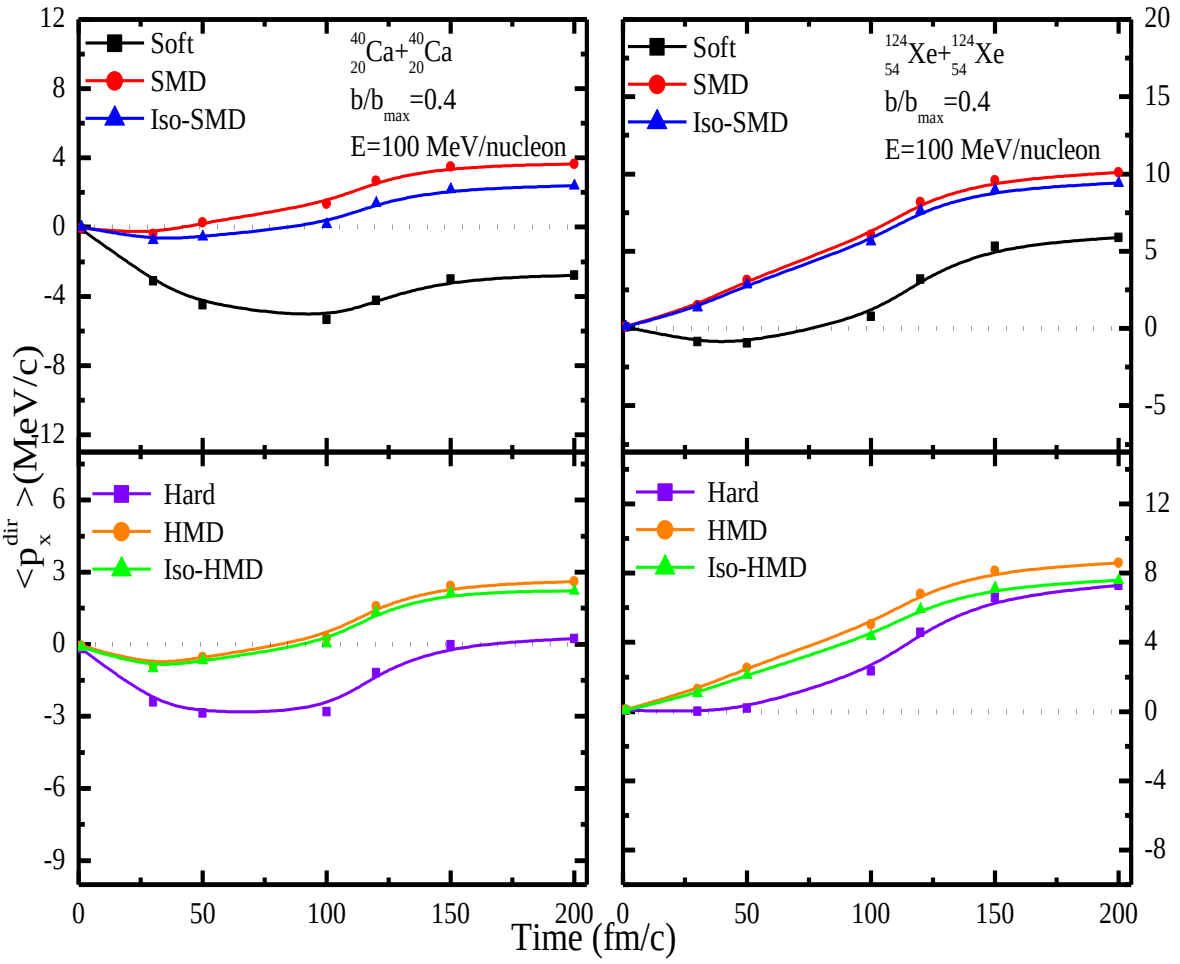

Fig. 3.8: The time evolution of $\left\langle p_x^{dir} \right\rangle$ for the reactions ^{40}Ca+^{40}Ca (left panels) and ^{124}Xe+^{124}Xe (right panels) at colliding geometry (b/b$_{max}$=0.4) at energy 100 MeV/nucleon.

3.4.4 Energy Dependence of directed flow for different systems

To study the influence of isospin momentum dependent interactions (Iso-MDI) on directed transverse flow or alternatively on the balance energy, in Figs. 3.9 and Fig. 3.10, incident energy dependence of the directed flow is displayed for different systems. The different lines in the figures represents the different equation of states. Here we perform the simulations with different EOS (soft and hard). Fig. 3.9: is for soft EOS and Fig. 3.10: represents the result for hard EOS for different systems. The directed flow changes from negative to positive value with an increase in the incident energy. This is the general trend and is explained many times in the literature by taking the concept of mean field and NN cross-section. One can reveal the following important results from the Figs. 3.9 and 3.10. First is, the transverse momentum increases monotonically with the increase in the incident energy. Momentum dependent interactions are repulsive in nature. For SMD and HMD EOS $\left\langle p_x^{dir} \right\rangle$ increase sharply. But when isospin degree of freedom is introduced in MDI there is reduction in $\left\langle p_x^{dir} \right\rangle$. Due to different strength of nn, np and pp cross sections, additional repulsion is produced. This additional repulsion will force the directed flow to make an earlier transition from negative to positive value and hence will lower the balance energy.

3.4.5 Balance Energy as a function of system mass

For the present study, we simulate several thousands of events of each reaction at incident energies around E_{bal} in small steps of 10 MeV/nucleon for each isotopic system of Ca+Ca and Xe+Xe. Here we study the mass dependence of balance energy for isotopic series of Ca

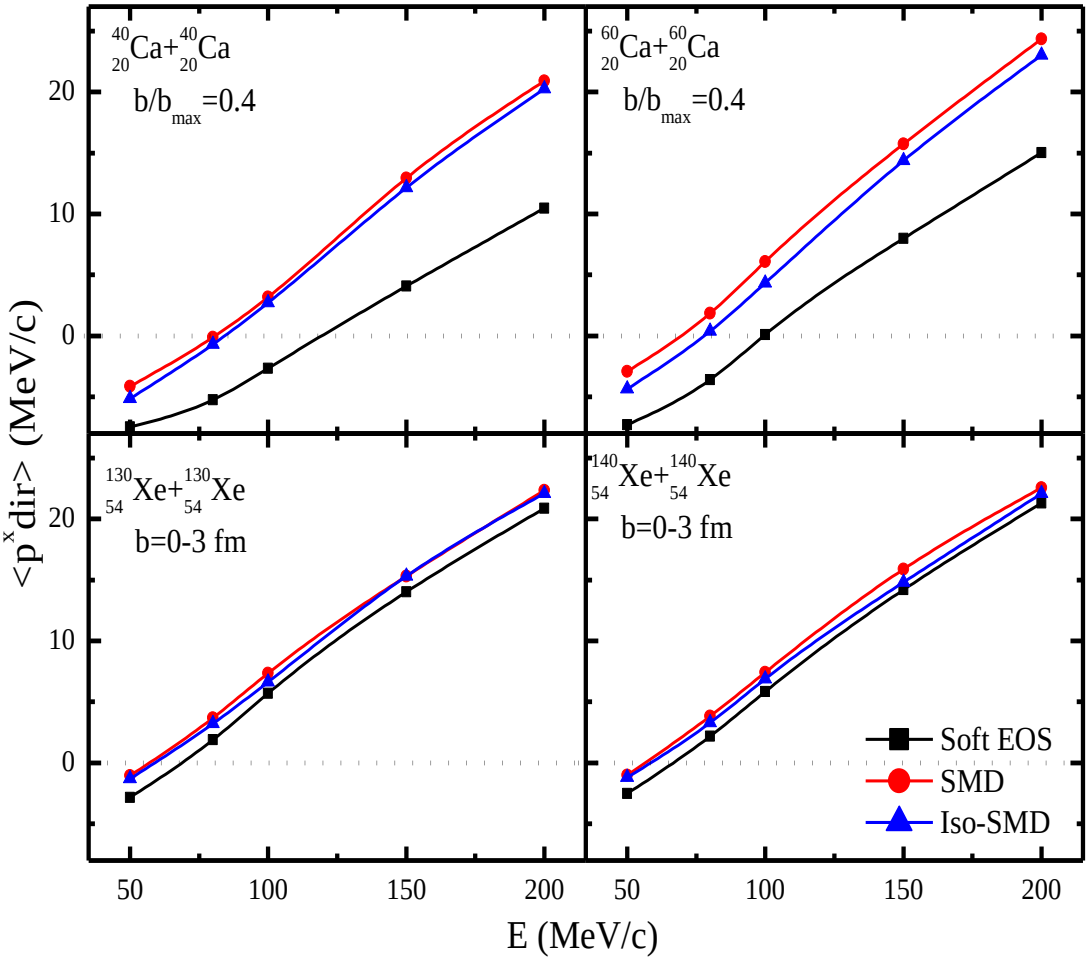

Fig. 3.9: Energy dependence of the directed nuclear flow $\left\langle p_x^{dir} \right\rangle$ for different systems. The different lines in the figure represent the directed flow for different soft equation of state i.e. Soft, SMD and Iso-SMD EOS.

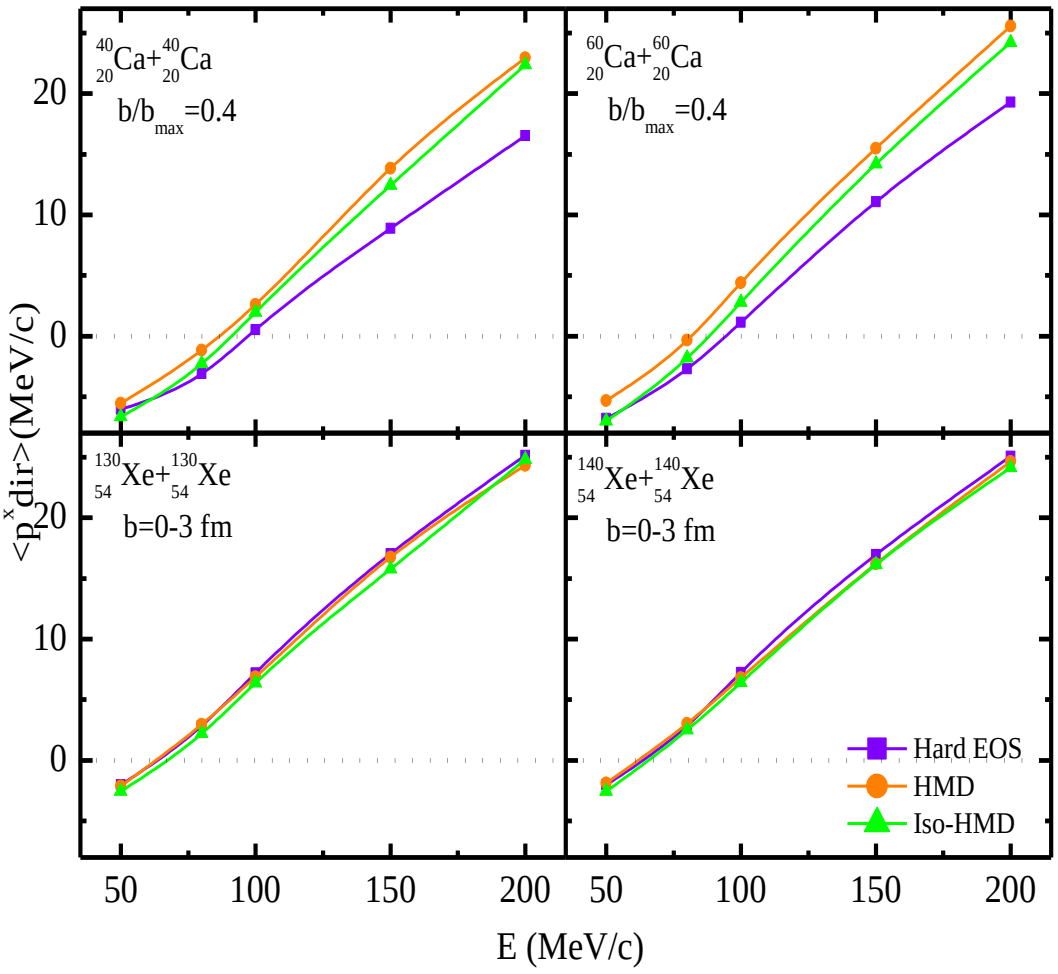

Fig. 3.10: Energy dependence of the directed nuclear flow $\left\langle p_x^{dir} \right\rangle$ for different systems. The different lines in the figure represent the directed flow for different hard equation of state i.e. Hard, HMD and Iso-HMD EOS.

having N/Z (N/A) varying from 1.0 to 2.0 (0.5-0.67) and of Xe having N/Z (N/A) varying from 1.2 to 1.6 (0.55-0.6). The N/A for a given pair is varied by adding neutron content only keeping the charge fixed, so that the effect of the Coulomb potential is same for a given mass pair. However this will lead to the increase in mass of systems with higher neutron content. We used soft and hard equation of states i.e. Soft, SMD, Iso-SMD, Hard, HMD, Iso-HMD. In Fig.s 3.11 and 3.12, we display the E_{bal} as a function of combined mass for different soft and hard equation of states. Fig.s 3.11 and 3.12 represent the solid black, red and blue lines represent E_{bal} as a function of combined mass for soft, SMD and Iso-SMD equation of states and similarly violet, orange and green solid lines represent E_{bal} as a function of combined mass for hard, HMD and Iso-HMD equation of states. Lines are linear fit to E_{bal}. As the mass of the system increases the value of E_{bal} decreases as shown in graphs. It has been found that MDI affects drastically the directed transverse flow as well as its disappearance but mass dependence of E_{bal} remains unchanged. While we introduced isospin degree of freedom in MDI there is a great reduction in the balance energy with respect to the MDI but also E_{bal} dependence of mass remains unchanged on inclusion of Iso-MDI. It shows a dependence of E_{bal} on Iso-MDI and symmetry potential. Role of MDI and Iso-MDI is stronger for lighter nuclei like in Fig. 3.11 for Ca isotopic series there is a huge difference between E_{bal} for all equation of states. But for heavier systems like Xe isotopic series E_{bal} difference decreases for all equation of states. In Fig. 3.11 we compare our results with experimental data [42], clearly our results are follow the same trend as that of experimental data.

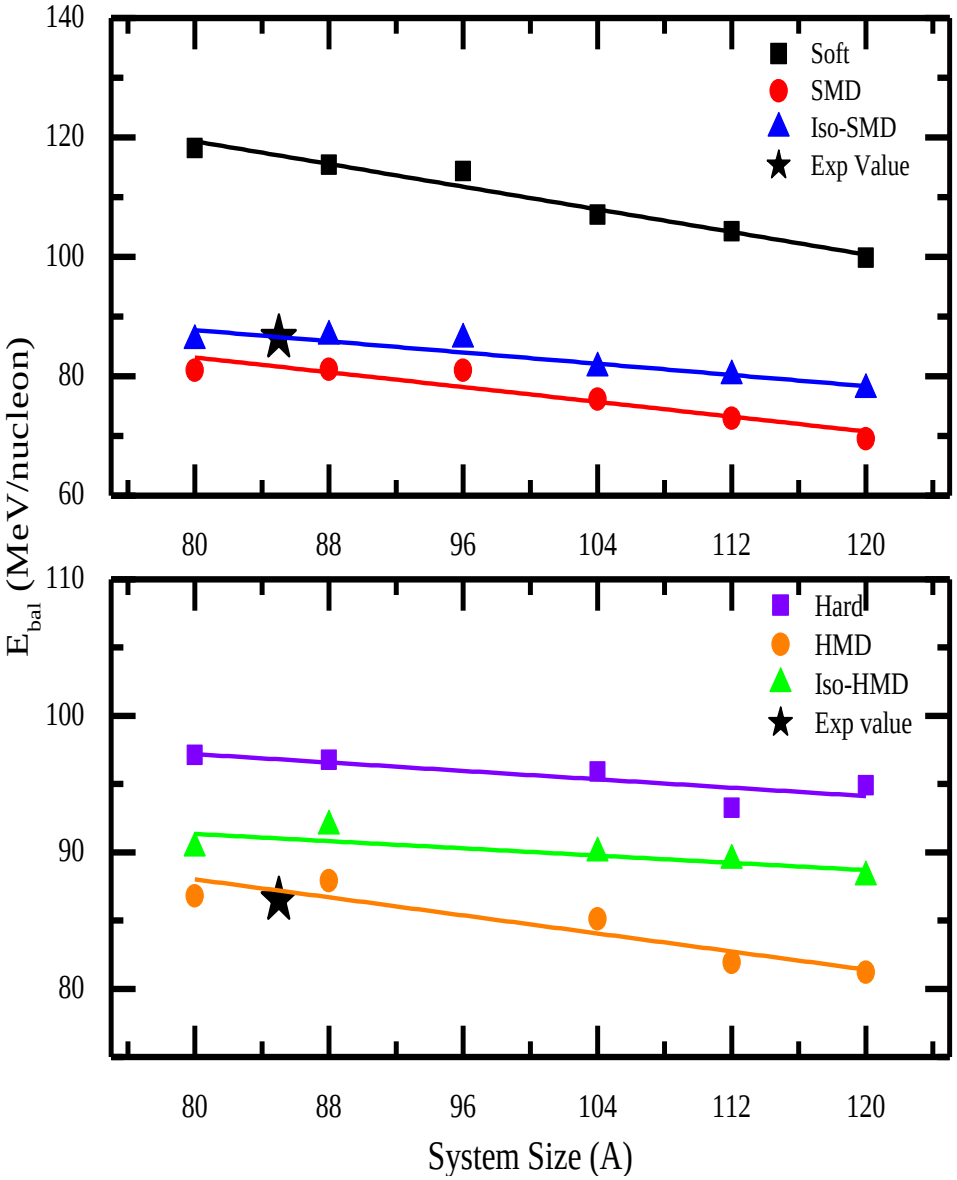

Fig. 3.11: E_{bal} as a function of combined mass of system for isotopic series of Ca . Various symbols and lines are explained in the text.

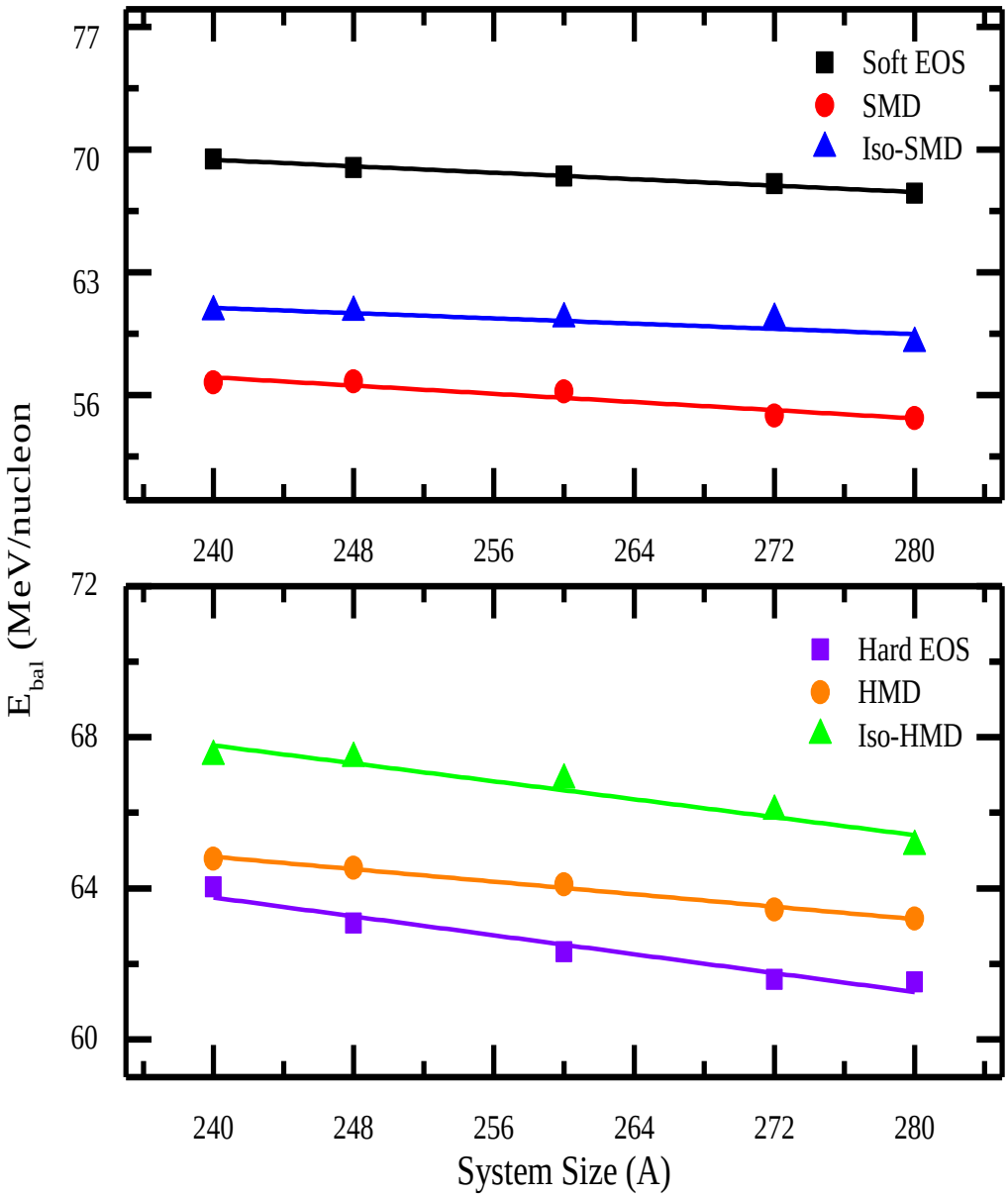

Fig. 3.12: E_{bal} as a function of combined mass of system for isotopic series of Xe. Various symbols and lines are explained in the text.

3.5 Summary

Using the IQMD model, we studied the role of different equation of states (soft and hard) with momentum dependent interactions (MDI), without MDI and with isospin momentum dependent interactions (Iso-MDI) on the directed flow and balance energy. A number of reactions were studied for isotopic series of Ca+Ca and isotopic series of Xe+Xe. The directed flow or in other words, balance energy is found to be sensitive towards the MDI and Iso-MDI. Our calculations with Iso-SMD follow the trend of experimental data. The dependence of MDI weakens with the increase in the size of the system. But there is a reduction in the balance energy in case of Iso-MDI from MDI because of the inclusion of isospin degree of freedom in MDI. Balance energy is higher for lower masses and lower for heavier masses. Balance energy followed a linear behavior with combined mass and decreases with increasing mass.

Directed flow is also sensitive towards the different impact parameters. MDI and Iso-MDI shows good effects at higher impact parameter as compared to lower one. Directed flow has more positive value for protons as compared to neutrons.

References

[1] R. B. Clare and D. Strottman. Phys. Rep. **141**, 179 (1986).

[2] Suneel Kumar, Ph. D. Thesis, P. U. Chandigarh, (1999).

[3] K. E. Zyromski et al., Phys. Rev. C **55**, R562 (1997).

[4] M. K. Sharma, Ph. D. Thesis, P. U. Chandigarh, (1998).

[5] H. Stocker and W. Greiner, Phys. Rep. **137**, 277 (1986).

[6] L. Shi, Ph. D thesis, MSU, USA (2003).

[7] B. K. Agrawal, R. Kumar, and S. K. Dhiman, Phys. Rev. D **77**, 087301 (2008).

[8] B. A. Li, C.M. Ko, Nucl. Phys. A **601**, 457 (1996).

[9] M. Demoulins et al., Phys. Lett. B **241**, 476 (1990).

[10] W. Schied, H. Muller and B. Zhang, Phys. Rev. Lett . **32**, 741 (1974).

[11] A. Insolia, U. Lombardo, N. G. Sandulescu and A. Bonasera, Phys. Lett. B **334**, 12 (1994).

[12] A. Andronic et al., Phys. Rev. C **67**, 034907(2003).

[13] J. Lukasik et al., Phys. Lett. B **608**, 223 (2005).

[14] E . Lehmann, A. Faessler, J. Zipprich, R. K. Puri and S. W. Huang, Z. Phys. A **355**, 55 (1996).

[15] H. Sorge, Phys. Rev. Lett. **78**, 2309 (1997).

[16] R. Pak et al., Phys. Rev. Lett. **78**, 1022 (1997); ibid. **78**, 1026 (1997).

[17] A. Andronic et al., Phys. Rev. C **64**, 041604(R) (2001).

[18] W. trautmann et al., Prog. Part. Nucl. Phys. **62**, 425 (2009).

[19] W. Reisdorf et al., Nucl. Phys. A **848**, 366 (2010).

[20] Z. Kohley et al., Phys. Rev. C **83**, 044601 (2011).

[21] B. A. Li, Z. Z. Ren, C. M. Ko and S,.J. Yennello, Phys. Rev. Lett. **76**, 4492 (1996).

[22] L. W. Chen, F. S. Zhang and G. M. Jin, Phys. Rev. C **58**, 2283 (1998).

[23] B. A. Li, A. T. Sustich and B. Zhang, Phys. Rev. C **64**, 054604 (2001).

[24] M. Di Toro et al., Nucl. Phys. A **782**, 267c (2007).

[25] S. Gautam, R. Chugh, A. D. Sood, R. K. Puri, Ch. Hartnack and J. Aichelin, J. phys. G: Nucl. Part. Phys. **37**, 085102 (2010).

[26] A. D. Sood and R. K. Puri, Phys. Rev. C **69**, 054612 (2004).

[27] A. D. Sood and R. K. Puri, Eur. Phys. J. A **30**, 571 (2006).

[28] S. Gautam and A. D. Sood , Phys. Rev. C **82**, 014604 (2010).

[29] S. Gautam, A. D. Sood, R. K. Puri, and J. Aichelin, Phys. Rev. C **83**, 014603 (2011).

[30] S. Kumar, R. K. Puri and J. Aichelin, Phys. Rev. C **58**, 1618 (1998).

[31] J.J. Molitoris, H. Stocker and B. L. Winer, Phys. Rev. C **36**, 220 (1987).

[32] J. Cugnon and C. Volant, Z Phys. A **334**, 435 (1989).

[33] E. A. Uehling and G. E. Uhlenbeck, Phys. Rev. **43**, 552 (1933).

[34] B. A. Li and S. J. Yennello, Phys. Rev. C **52**, R1746 (1995).

[35] J. Aichelin, Phys. Reports, **202**, 233 (1991).

[36] C. Hartnack et al., Eur. Phys. J. A **1**, 151 (1998); C. Hartnack et al., Phys. Rep. **510**, 119 (2012).

[37] H. Kruse, B. V. Jacak, and H. Stocker. Phys. Rev. Lett. **54**, 289 (1985).

[38] J. Aichelin, A. rosenhaur, G. Peilert, H. Stocker, and W. Greier, Phys. Rev. Lett. **58**, 1926 (1987).

[39] S. Hama, B. C. Clark, E. D. Cooper, H. S. Sherif and R. L. Mercer, Phys. Rev. C **41**, 2737 (1990).

[40] J. Y. Liu, W. J. Guo, Z. Y. Xing, and X. G. Lee, Chin. Phys. Lett. **22**, 65 (2005).

[41] B. A. Li, C. B. Das, S. Das Gupta and C. Gale, Phys Rev. C **69**, 011603(R) (2004); B. A. Li, C. B. Das, S. D. Gupta, and C. Gale, Nucl. Phys. A **735**, 563 (2004).

[42] D. J. Magestro, W. Bauer, O. Bjarki, J. D. Crispin, M. L. Miller, M. B. Tonjes, A.M. Vander Molen, G. D. Westfall, R. Pak, and E. Norbeck, Phys. Rev. C **61**, 021602(R) (2000).